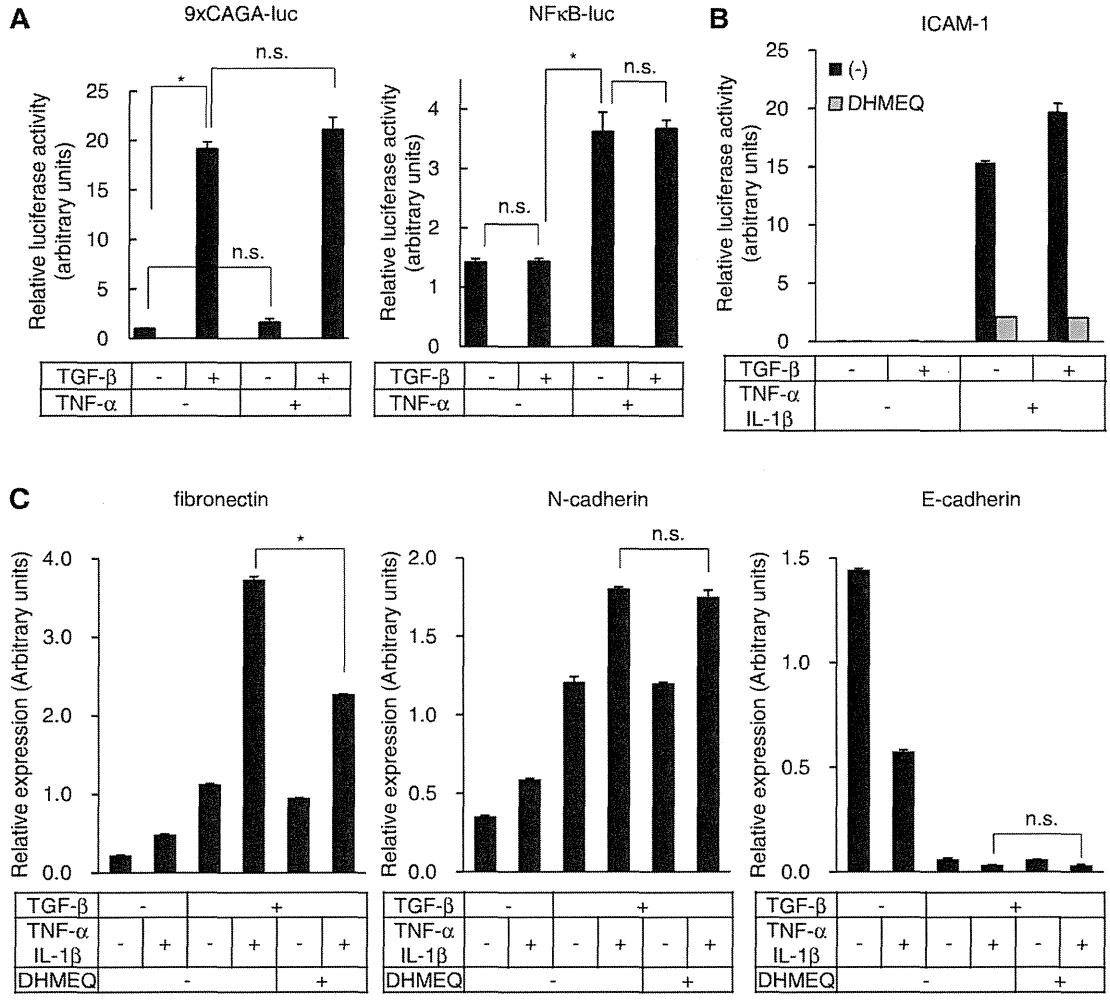

Fig. 7 Effect of DHMEQ on the enhancement of EMT marker expression by TNF-α and IL-1β. (A) A 9xCAGA-luc luciferase construct consisting of tandemly repeated Smad binding elements and NF-κB-luc luciferase reporter construct were transfected in A549 cells and stimulated with 5 ng/ml of TGF-β and 20 ng/ml of TNF-α for 24 h (9xCAGA-luc) or 6 h (NFκB-luc). (B) Inhibition of TNF-α and IL-1β-induced ICAM-1 expression by DHMEQ. A549 cells were pre-treated with 10 μg/ml of DHMEQ or DMSO as a control for 3.5 h and stimulated by TNF-α and IL-1β for 4 h. ICAM-1 expression was measured by qRT–PCR. (C) A549 cells were treated as in (B), and stimulated with TGF-β, TNF-α and IL-1β for 24 h. Expression of EMT markers was analysed by qRT–PCR. $*P<0.05$; Error bars, SDs; n.s., not significant.

TNF-α was observed only in the presence of TGF-β. Nevertheless, TGF-β-induced phosphorylation of Smad2, and Smad-induced 9xCAGA luciferase reporter activity did not change following the addition of TNF-α. We also observed that TGF-β does not enhance TNF-α-induced transcriptional activity of NFκB-luc, and that enhanced expression of target genes by TNF-α was selective to fibronectin and N-cadherin. Although many reports have revealed crosstalk between TNF-α and TGF-β signalling pathways in a variety of cells (*43*, *44*), the present analyses suggest that the cooperation of these cytokines appears to be exerted at the transcription level of each target gene depending on the context of their *cis*-regulatory elements, indicating differences in the transcriptional responses of target genes (*34*, *45*, *46*). Thus, neutralizing antibody against TNF-α inhibited the expression of both fibronectin and N-cadherin. In contrast, only the expression of fibronectin was inhibited by DHMEQ and U0126, whereas that of N-cadherin was inhibited by SB203580. Combinatorial effects of the several inhibitors on EMT phenotypes including expression of fibronectin and N-cadherin in the context of co-stimulation by TGF-β and inflammatory cytokines need to be evaluated in the future analyses.

The importance of EMT in cancer pathophysiology is not limited to cancer cell invasion and metastasis. Asiedu et al. reported generation of breast cancer stem cells by TNF-α and TGF-β (*47*). Based on our analyses suggesting the importance of TNF-α on TGF-β-induced EMT in A549 cells at a level of endogenous secretion from RAW 264.7 cells, complex mechanisms of enhancement by TNF-α require further examination to develop methods for controlling tumour cell invasion and cancer stem cells.

Supplementary Data

Supplementary Data are available at *JB* online.

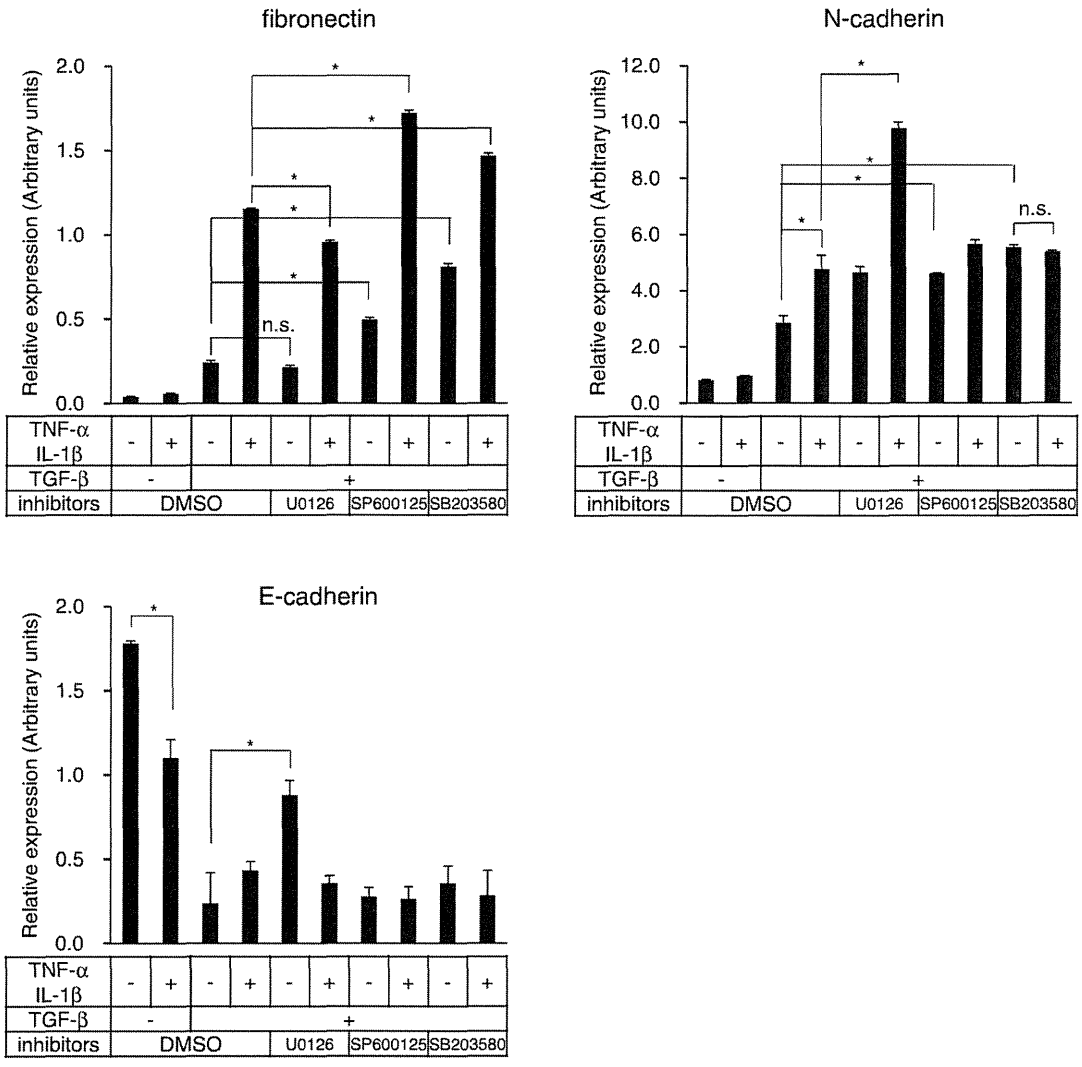

Fig. 8 Effect of kinase inhibitors on enhancement of TGF-β-induced EMT by TNF-α and IL-1β. A549 cells were pre-treated with either 10 μM U0126 (MEK inhibitor), 1 μM SP600125 (JNK inhibitor) or 1 μM SB203580 (p38 inhibitor) for 3.5 h. Cells were then stimulated with 5 ng/ml TGF-β, 20 ng/ml TNF-α and 1 ng/ml IL-1β for 24 h. Expression of EMT markers was determined by qRT–PCR after 24-h stimulation and normalized by GAPDH. $*P<0.05$; Error bars, SDs; n.s., not significant.

Acknowledgements

The authors thank Keiko Yuki and Yasuyuki Morishita for technical assistance.

Funding

KAKENHI [Grants-in-aid for Scientific Research on Innovative Areas (Integrative Research on Cancer Microenvironment Network grant 22112002 to K.M.) and for young scientists (B) (22790750 to D.K.)] from the Ministry of Education, Culture, Sports, Science, and Technology of Japan (MEXT); the Global Center of Excellence Program (Integrative Life Science Based on the Study of Biosignaling Mechanisms) from the Japan Society for the Promotion of Science.

Conflict of interest

None declared.

References

1. Bierie, B. and Moses, H.L. (2006) Tumour microenvironment: TGF-β: the molecular Jekyll and Hyde of cancer. *Nat. Rev. Cancer* **6**, 506–520
2. Ikushima, H. and Miyazono, K. (2010) TGF-β signalling: a complex web in cancer progression. *Nat. Rev. Cancer* **10**, 415–424
3. Yoshimura, A., Wakabayashi, Y., and Mori, T. (2010) Cellular and molecular basis for the regulation of inflammation by TGF-β. *J. Biochem.* **147**, 781–792
4. Derynck, R., Akhurst, R.J., and Balmain, A. (2001) TGF-β signaling in tumor suppression and cancer progression. *Nat. Genet.* **29**, 117–129
5. Sabe, H. (2011) Cancer early dissemination: cancerous epithelial-mesenchymal transdifferentiation and transforming growth factor-β signalling. *J. Biochem.* **149**, 633–639
6. Miyazono, K. (2009) Transforming growth factor-β signaling in epithelial-mesenchymal transition and progression of cancer. *Proc. Jpn. Acad. Ser. B Phys. Biol. Sci.* **85**, 314–323
7. Meulmeester, E. and ten Dijke, P. (2011) The dynamic roles of TGF-β in cancer. *J. Pathol.* **223**, 205–218
8. Heldin, C.H., Miyazono, K., and ten Dijke, P. (1997) TGF-β signalling from cell membrane to nucleus through SMAD proteins. *Nature* **390**, 465–471

9. Miyazono, K., Kamiya, Y., and Morikawa, M. (2010) Bone morphogenetic protein receptors and signal transduction. *J. Biochem.* **147**, 35–51
10. Thuault, S., Valcourt, U., Petersen, M., Manfioletti, G., Heldin, C.H., and Moustakas, A. (2006) Transforming growth factor-β employs HMGA2 to elicit epithelial-mesenchymal transition. *J. Cell Biol.* **174**, 175–183
11. Shirakihara, T., Saitoh, M., and Miyazono, K. (2007) Differential regulation of epithelial and mesenchymal markers by δEF1 proteins in epithelial mesenchymal transition induced by TGF-β. *Mol. Biol. Cell* **18**, 3533–3544
12. Kondo, M., Cubillo, E., Tobiume, K., Shirakihara, T., Fukuda, N., Suzuki, H., Shimizu, K., Takehara, K., Cano, A., Saitoh, M., and Miyazono, K. (2004) A role for Id in the regulation of TGF-β-induced epithelial-mesenchymal transdifferentiation. *Cell Death Differ.* **11**, 1092–1101
13. Vincent, T., Neve, E.P., Johnson, J.R., Kukalev, A., Rojo, F., Albanell, J., Pietras, K., Virtanen, I., Philipson, L., Leopold, P.L., Crystal, R.G., de Herreros, A.G., Moustakas, A., Pettersson, R.F., and Fuxe, J. (2009) A SNAIL1-SMAD3/4 transcriptional repressor complex promotes TGF-β mediated epithelial-mesenchymal transition. *Nat. Cell Biol.* **11**, 943–950
14. Thuault, S., Tan, E.J., Peinado, H., Cano, A., Heldin, C.H., and Moustakas, A. (2008) HMGA2 and Smads co-regulate SNAIL1 expression during induction of epithelial-to-mesenchymal transition. *J. Biol. Chem.* **283**, 33437–33446
15. Morita, T., Mayanagi, T., and Sobue, K. (2007) Dual roles of myocardin-related transcription factors in epithelial mesenchymal transition via slug induction and actin remodeling. *J. Cell Biol.* **179**, 1027–1042
16. Mihira, H., Suzuki, H., Akatsu, Y., Yoshimatsu, Y., Igarashi, T., Miyazono, K., and Watabe, T. (2011) TGF-β-induced mesenchymal transition of MS-1 endothelial cells requires Smad-dependent cooperative activation of Rho signals and MRTF-A. *J. Biochem.*, doi:10.1093/jb/mvr121
17. Saito, R.A., Watabe, T., Horiguchi, K., Kohyama, T., Saitoh, M., Nagase, T., and Miyazono, K. (2009) Thyroid transcription factor-1 inhibits transforming growth factor-β-mediated epithelial-to-mesenchymal transition in lung adenocarcinoma cells. *Cancer Res.* **69**, 2783–2791
18. Moustakas, A. and Heldin, C.H. (2007) Signaling networks guiding epithelial-mesenchymal transitions during embryogenesis and cancer progression. *Cancer Sci.* **98**, 1512–1520
19. Shirakihara, T., Horiguchi, K., Miyazawa, K., Ehata, S., Shibata, T., Morita, I., Miyazono, K., and Saitoh, M. (2011) TGF-β regulates isoform switching of FGF receptors and epithelial-mesenchymal transition. *EMBO J.* **30**, 783–795
20. Maier, H.J., Schmidt-Strassburger, U., Huber, M.A., Wiedemann, E.M., Beug, H., and Wirth, T. (2010) NF-κB promotes epithelial-mesenchymal transition, migration and invasion of pancreatic carcinoma cells. *Cancer Lett.* **295**, 214–228
21. Borthwick, L.A., McIlroy, E.I., Gorowiec, M.R., Brodlie, M., Johnson, G.E., Ward, C., Lordan, J.L., Corris, P.A., Kirby, J.A., and Fisher, A.J. (2010) Inflammation and epithelial to mesenchymal transition in lung transplant recipients: role in dysregulated epithelial wound repair. *Am. J. Transplant.* **10**, 498–509
22. Kasai, H., Allen, J.T., Mason, R.M., Kamimura, T., and Zhang, Z. (2005) TGF-β1 induces human alveolar epithelial to mesenchymal cell transition (EMT). *Respir. Res.* **6**, 56
23. Umezawa, K., Ariga, A., and Matsumoto, N. (2000) Naturally occurring and synthetic inhibitors of NF-κB functions. *Anticancer Drug Des.* **15**, 239–244
24. Matsumoto, N., Ariga, A., To-e, S., Nakamura, H., Agata, N., Hirano, S., Inoue, J., and Umezawa, K. (2000) Synthesis of NF-κB activation inhibitors derived from epoxyquinomicin C. *Bioorg. Med. Chem. Lett.* **10**, 865–869
25. Nagano, Y., Koinuma, D., Miyazawa, K., and Miyazono, K. (2010) Context-dependent regulation of the expression of c-Ski protein by Arkadia in human cancer cells. *J. Biochem.* **147**, 545–554
26. Horiguchi, K., Shirakihara, T., Nakano, A., Imamura, T., Miyazono, K., and Saitoh, M. (2009) Role of Ras signaling in the induction of snail by transforming growth factor-β. *J. Biol. Chem.* **284**, 245–253
27. Nagata, M., Nagata, S., Yuki, K., Isogaya, K., Saitoh, M., Miyazono, K., and Miyazawa, K. (2010) Identification of a phosphorylation site in c-Ski as serine 515. *J. Biochem.* **148**, 423–427
28. Mizutani, A., Saitoh, M., Imamura, T., Miyazawa, K., and Miyazono, K. (2010) Arkadia complexes with clathrin adaptor AP2 and regulates EGF signalling. *J. Biochem.* **148**, 733–741
29. Soll, D.R., Voss, E., Varnum-Finney, B., and Wessels, D. (1988) "Dynamic Morphology System": a method for quantitating changes in shape, pseudopod formation, and motion in normal and mutant amoebae of Dictyostelium discoideum. *J. Cell. Biochem.* **37**, 177–192
30. Katsuno, Y., Hanyu, A., Kanda, H., Ishikawa, Y., Akiyama, F., Iwase, T., Ogata, E., Ehata, S., Miyazono, K., and Imamura, T. (2008) Bone morphogenetic protein signaling enhances invasion and bone metastasis of breast cancer cells through Smad pathway. *Oncogene* **27**, 6322–6333
31. Nakano, A., Koinuma, D., Miyazawa, K., Uchida, T., Saitoh, M., Kawabata, M., Hanai, J., Akiyama, H., Abe, M., Miyazono, K., Matsumoto, T., and Imamura, T. (2009) Pin1 down-regulates transforming growth factor-β (TGF-β) signaling by inducing degradation of Smad proteins. *J. Biol. Chem.* **284**, 6109–6115
32. Dennler, S., Itoh, S., Vivien, D., ten Dijke, P., Huet, S., and Gauthier, J.M. (1998) Direct binding of Smad3 and Smad4 to critical TGF-β-inducible elements in the promoter of human plasminogen activator inhibitor-type 1 gene. *EMBO J.* **17**, 3091–3100
33. Lernbecher, T., Muller, U., and Wirth, T. (1993) Distinct NF-κ B/Rel transcription factors are responsible for tissue-specific and inducible gene activation. *Nature* **365**, 767–770
34. Mizutani, A., Koinuma, D., Tsutsumi, S., Kamimura, N., Morikawa, M., Suzuki, H.I., Imamura, T., Miyazono, K., and Aburatani, H. (2011) Cell-type specific target selection by combinatorial binding of Smad2/3 and hepatocyte nuclear factor 4-α in HepG2 cells. *J. Biol. Chem.* **286**, 29848–29860
35. Liu, X. (2008) Inflammatory cytokines augments TGF-β1-induced epithelial-mesenchymal transition in A549 cells by up-regulating TβR-I. *Cell Motil. Cytoskeleton* **65**, 935–944
36. Kim, J.H., Jang, Y.S., Eom, K.S., Hwang, Y.I., Kang, H.R., Jang, S.H., Kim, C.H., Park, Y.B., Lee, M.G., Hyun, I.G., Jung, K.S., and Kim, D.G. (2007)

Transforming growth factor β1 induces epithelial-to-mesenchymal transition of A549 cells. *J. Korean Med. Sci.* **22**, 898–904

37. Yamauchi, Y., Kohyama, T., Takizawa, H., Kamitani, S., Desaki, M., Takami, K., Kawasaki, S., Kato, J., and Nagase, T. (2010) Tumor necrosis factor-α enhances both epithelial-mesenchymal transition and cell contraction induced in A549 human alveolar epithelial cells by transforming growth factor-β1. *Exp. Lung Res.* **36**, 12–24
38. Camara, J. and Jarai, G. (2010) Epithelial-mesenchymal transition in primary human bronchial epithelial cells is Smad-dependent and enhanced by fibronectin and TNF-α. *Fibrogenesis Tissue Repair* **3**, 2
39. Kamitani, S., Yamauchi, Y., Kawasaki, S., Takami, K., Takizawa, H., Nagase, T., and Kohyama, T. (2011) Simultaneous stimulation with TGF-β1 and TNF-α induces epithelial mesenchymal transition in bronchial epithelial cells. *Int. Arch. Allergy Immunol.* **155**, 119–128
40. Schulz, C., Farkas, L., Wolf, K., Kratzel, K., Eissner, G., and Pfeifer, M. (2002) Differences in LPS-induced activation of bronchial epithelial cells (BEAS-2B) and type II-like pneumocytes (A-549). *Scand. J. Immunol.* **56**, 294–302
41. Tsutsumi-Ishii, Y. and Nagaoka, I. (2003) Modulation of human β-defensin-2 transcription in pulmonary epithelial cells by lipopolysaccharide-stimulated mononuclear phagocytes via proinflammatory cytokine production. *J. Immunol.* **170**, 4226–4236
42. Kim, S., Takahashi, H., Lin, W.W., Descargues, P., Grivennikov, S., Kim, Y., Luo, J.L., and Karin, M. (2009) Carcinoma-produced factors activate myeloid cells through TLR2 to stimulate metastasis. *Nature* **457**, 102–106
43. Takahashi, E., Nagano, O., Ishimoto, T., Yae, T., Suzuki, Y., Shinoda, T., Nakamura, S., Niwa, S., Ikeda, S., Koga, H., Tanihara, H., and Saya, H. (2010) Tumor necrosis factor-α regulates transforming growth factor-β-dependent epithelial-mesenchymal transition by promoting hyaluronan-CD44-moesin interaction. *J. Biol. Chem.* **285**, 4060–4073
44. Bitzer, M., von Gersdorff, G., Liang, D., Dominguez-Rosales, A., Beg, A.A., Rojkind, M., and Bottinger, E.P. (2000) A mechanism of suppression of TGF-β/SMAD signaling by NF-κ B/RelA. *Genes Dev.* **14**, 187–197
45. Gomis, R.R., Alarcon, C., He, W., Wang, Q., Seoane, J., Lash, A., and Massague, J. (2006) A FoxO-Smad synexpression group in human keratinocytes. *Proc. Natl. Acad. Sci. USA* **103**, 12747–12752
46. Koinuma, D., Tsutsumi, S., Kamimura, N., Taniguchi, H., Miyazawa, K., Sunamura, M., Imamura, T., Miyazono, K., and Aburatani, H. (2009) Chromatin immunoprecipitation on microarray analysis of Smad2/3 binding sites reveals roles of ETS1 and TFAP2A in transforming growth factor β signaling. *Mol. Cell. Biol.* **29**, 172–186
47. Asiedu, M.K., Ingle, J.N., Behrens, M.D., Radisky, D.C., and Knutson, K.L. (2011) TGF-β/TNF-α-mediated epithelial-mesenchymal transition generates breast cancer stem cells with a claudin-low phenotype. *Cancer Res.* **71**, 4707–4719

Induced lymphatic sinus hyperplasia in sentinel lymph nodes by VEGF-C as the earliest premetastatic indicator

RUEDIGER LIERSCH[1,2,3], SATOSHI HIRAKAWA[1], WOLFGANG E. BERDEL[2], ROLF M. MESTERS[2] and MICHAEL DETMAR[1,3]

[1]Cutaneous Biology Research Center, Massachusetts General Hospital and Harvard Medical School, Charlestown, MA 02129, USA; [2]Department of Medicine A, Hematology and Oncology, University of Muenster, Albert-Schweitzer Campus, D-48129 Muenster, Germany; [3]Institute of Pharmaceutical Sciences, Swiss Federal Institute of Technology (ETH), 8092 Zurich, Switzerland

Received February 23, 2012; Accepted May 17, 2012

DOI: 10.3892/ijo.2012.1665

Abstract. Research on tumor-induced lymphangiogenesis has predominantly focused on alterations and abnormal growth of peritumoral and intratumoral lymphatic vessels. However, recent evidence indicates that lymphangiogenesis of sentinel lymph nodes might also contribute to cancer progression. In clinical oncology, the sentinel lymph nodes play an important role in diagnosis, staging and management of disease. The prognostic value that may be placed in the analysis of various parameters in tumor-free lymph nodes is still under debate. We, therefore, chose to investigate genetically fluorescent MDA-MB-435/green fluorescent protein human cancer cells transfected to overexpress VEGF-C in a nude mouse model and investigated metastasis, lymph node lymphangiogenesis, lymph node angiogenesis and size of sentinel lymph nodes. The nature of MDA-MB-435, identified as a breast cancer cell line for several decades, has recently been reidentified as being from melanoma origin. Vascular endothelial growth factor-C overexpression induced early metastasis and significantly increased the lymphatic vessel area in sentinel lymph nodes even before the tumor metastasis. At early timepoints, expansion of the lymphatic network was observed even though no difference of blood vessel area and lymph node size was detected. These results suggest that primary tumors -via secretion of VEGF-C- can induce hyperplasia of the sentinel lymph node lymphatic vessel network and thereby promote their further spread. In cases of tumor-free lymph nodes the increased lymphatic network of sentinel lymph nodes is a very early premetastatic sign and may provide a new prognostic indicator and target for aggressive diseases.

Correspondence to: Dr Ruediger Liersch, Department of Medicine A, Hematology and Oncology, University of Muenster, Albert-Schweitzer-Campus 1, D-48149 Muenster, Germany
E-mail: rliersch@uni-muenster.de

Key words: metastasis, sentinel lymph node, VEGF-C, lymphatic sinuses, lymphatic endothelial cells

Introduction

Tumor-induced lymphangiogenesis has primarily been investigated concentrating on peritumoral and intratumoral lymphatic vessels at primary sites. Studies in animal tumor models have shown that lymphatic vessels promote the metastatic spread of tumors (1-3), and that the induction of lymphangiogenesis could even be used as a prognostic indicator for metastatic risk of human malignant melanoma of the skin (4). The vascular endothelial growth factors (VEGF)-C and -D have been identified as factors predominantly lymphangiogenic via the VEGF receptor-3 (VEGFR-3) (5). Studies have shown that this receptor is expressed on lymphatic endothelial cells of lymphatic vessels (5) and on lymphatic sinuses within lymph nodes (6). Moreover, it has been shown that blocking VEGFR-3 signaling can decrease tumor lymphangiogenesis and cancer spread (7-9).

Previously, were able to show that lymphangiogenesis of sentinel lymph nodes might also play a role in cancer progression. VEGF-A and VEGF-C expressing skin tumors maintained their lymphangiogenic activity after metastasizing to the sentinel lymph node and even induced sentinel lymph node (LN) lymphangiogenesis before the tumor has metastasized (10,11). LN-lymphangiogenesis was also identified in melanoma models after subcutaneous implantation prior to metastasis (12).

In clinical oncology, the sentinel lymph nodes play an important role in diagnosis, staging and management of disease. Especially in breast cancer and melanoma the involvement of regional lymph nodes is an excellent prognostic indicator. But about two thirds of the invasive cancers have no regional lymph node involvement and of those another third will recur (13,14). Studies evaluating the prognostic value of tumor-free sentinel lymph nodes are contradictory (15-17).

Lymph nodes constitute a critical crossroad between drained proteins, antigen-presenting cells, lymphocytes and even tumor cells. Also in the absence of tumor metastasis draining lymph nodes can undergo hyperplasia in number and size (18), because an immune response is also associated with changes of various parameters, such as fluid accumulation, migration and proliferation (19,20).

To investigate the earliest changes of the sentinel lymph nodes we injected genetically modified fluorescent MDA-MB-435/green fluorescent protein human melanoma cancer cells transfected to overexpress VEGF-C or control vector in nude mice. The MDA-MB-435 cell line, which has been reclassified from breast to melanoma, has been derived from the M14 melanoma cell line (21,22). In tumor-free sentinel lymph nodes we determined the lymphangiogenesis, angiogenesis and lymph node size of sentinel lymph nodes. VEGF-C overexpression significantly induced lymphatic sinus hyperplasia in sentinel lymph nodes even before the tumor metastasis. At early timepoints, the expansion of the lymphatic network was observed even though no difference of blood vessel area and lymph node size was detected. These results suggest that primary tumors, via secretion of lymphangiogenic factors, can induce hyperplasia of the sentinel lymph node lymphatic network and in case of tumor free non-enlarged lymph nodes might provide a new prognostic indicator.

Materials and methods

Cell lines. As tumor cells we used a previously published cell line (1). The MDA-MB-435 cell line, which has been reclassified from breast to melanoma, was derived from the M14 melanoma cell line (21, 22). The two MDA-MB-435 cell lines (American Type Culture Collection, Rockville, MD, USA) were grown in DMEM with 10% fetal bovine serum (FBS) and transfected with the expression construct (pcDNA3.1/EGFP) using the Superfect reagent (Qiagen, Chatsworth, CA, USA). Clone 6 had the highest tumor take and produced lymph node and lung metastasis. Clone 6 was transfected with the human VEGF-C cDNA (23) into a pcDNA3.1/ZEO vector. The transfected cell lines were maintained in media containing 600 μg/ml zeocin and 400 μg/ml geneticin. All animal studies were approved by the Massachusetts General Hospital Subcommittee on Research Animal Care.

Metastasis assay. Cells were injected bilaterally into the second mammary fat pads of athymic, female, eight-week-old NCR nu/nu mice ($2x10^6$ cells/100 μl serum-free culture medium). Two mice of each group (VEGF-C transfected MDA-MB-435 and control vector transfected MDA-MB-435) were sacrificed every two weeks until week ten. The two sentinel lymph nodes and the superficial inguinal lymph nodes were removed from each mouse and paraffin embedded (24). Tumor volume was determined as previously published (25). The smallest and largest tumor diameter were measured every other week, using a digital caliper, and tumor volumes were calculated using the following formula: volume = 4/3 x (1/2 x smaller diameter)2 x 1/2 x larger diameter. Tumor data were statistically analyzed by the two-sided unpaired t-test.

Immunostainings and immunofluorescence analysis. Sections were stained using antibodies to mouse LYVE-1 (kindly provided by Dr D. Jackson, Oxford, UK; Upstate Biotechnology, Lake Placid, NY, USA), CD31 (BD Biosciences Pharmingen, San Diego, CA, USA), Prox-1 (Covance, Berkeley, CA, USA), F4/80 (Serotech, Raleigh, NC, USA) and corresponding secondary antibodies labeled with Alexa Fluor 488 or 594 (Molecular Probes, Eugene, OR, USA). Cell nuclei were counterstained with Hoechst-bisbenzimide (Sigma-Aldrich). Specimens were examined by using a Nikon E-600 microscope (Nikon, Melville, NY, USA) and images captured with a SPOT digital camera (Diagnostic Instruments, Sterling Heights, MI, USA). At autopsy, all axillary and inguinal lymph nodes were examined for the presence of metastases. In addition, we determined the presence of metastases by fluorescence microscopic analysis and H&E staining for each lymph node.

Computer-assisted lymph node and lymphatic/medullary sinuses analysis. Representative H&E stained slides of the inguinal and axillary lymph nodes, obtained from the two groups (n=10 for each group) and 4 controls, were analyzed for the highest diameter, sections were examined by a Nikon E-600 microscope (Nikon) and images captured with a SPOT digital camera (Diagnostic Instruments). Further sections were stained with lymphatic and blood vessel markers (LYVE-1/CD31) to examine the lymphatic and blood vessel network. Images were captured with a Spot digital camera (Diagnostic Instruments). Computer-assisted morphometric analyses of the lymph node size, lymphatic network (lymphatic plus medullary sinuses) and blood vessel area were performed using the IP-LAB software (Scanalytics, Billerica, MA, USA). Statistical analyses were performed using the two-sided, unpaired Student's t-test.

Results

Lymphatic endothelial markers of the lymph node sinus endothelium. For distinguishing lymphatic endothelium from blood vessel endothelium in lymph nodes for computer-assisted evaluation we identified the lymphatic endothelial cell expression profile. We investigated the expression of known lymphatic markers, using antibodies against Lyve-1, Prox-1 and PECAM-1 (Fig. 1) (reviewed in ref. 26). The lymph node consists of a lymphatic labyrinth filled with lymphocytes (27). Within the lymph node the afferent lymphatic vessel enters the capsule and empties into the subcapsular sinus, which is connected to the trabecular and medullary sinuses (Fig. 1) (28,29). It could be shown that those sinuses are lined with a continued endothelium with long and elaborate intercellular junctions supported by reticular cells (30). Immunofluorescence staining revealed that the lining endothelium of the subcaspsular, lymphatic and medullary sinuses express a lymphatic endothelial profile. Lining endothelium is positive for Lyve-1 (Fig. 1A and B) and Prox-1 (Fig. 1C and D, arrow). Especially, the expression of the most reliable marker for lymphatic endothelial cells, Prox-1, revealed the lymphatic phenotype of the lining endothelium.

Lymphatic sinuses of the cortical and paracortical zone are indicated by the asterisk (Fig. 1A and B). Interestingly, the lymphatic sinuses and medullary sinuses were in close proximity to the high endothelial venules (Fig. 1A and B, arrowhead), but we detected no direct communication.

VEGF-C does not significantly increase the size of the sentinel lymph nodes. To investigate the effect of VEGF-C on tumor growth and sentinel lymph node size we used the previously published human cell line MDA-MB-435 transfected with human VEGF-C (1). We examined the growth of the tumor volume (Fig. 2A) and found that the average tumor growth rate revealed no significant difference between the VEGF-C transfected and

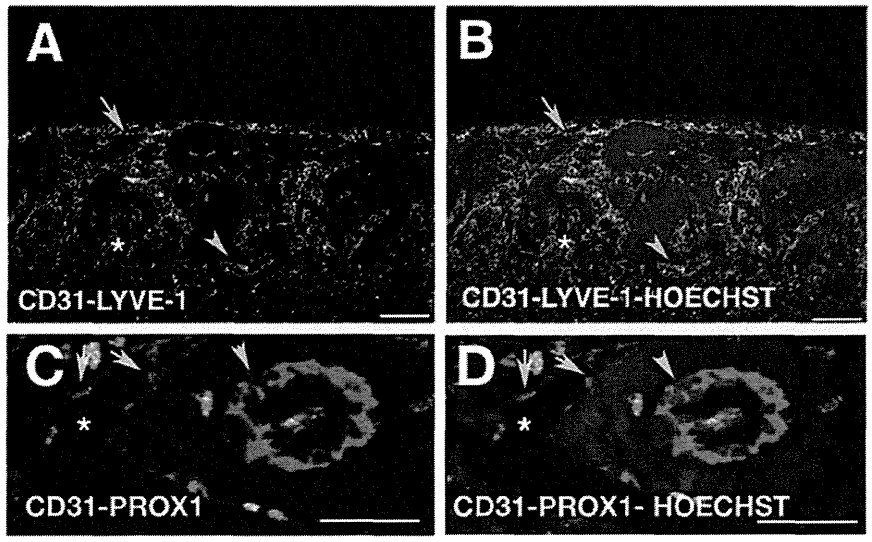

Figure 1. Lymphatic sinuses of lymph nodes express Prox-1. Immunofluorescence staining for LYVE-1, Prox-1 and CD31 depict lymphatic endothelial cells of lymphatic/medullary sinuses and blood vessels in the cortical and paracortical zone of sentinel lymph nodes. (A and B) *Medullary sinuses positive for LYVE-1 (A, green) and high endothelial venules positive for CD31 (A, red, arrowhead). (C and D) *Medullary sinuses positive for Prox-1 (C, green nuclei) and high endothelial venules positive for CD31 (A, red, arrowhead); A and B, scale bar 100 μm; C and D, scale bar 50 μm.

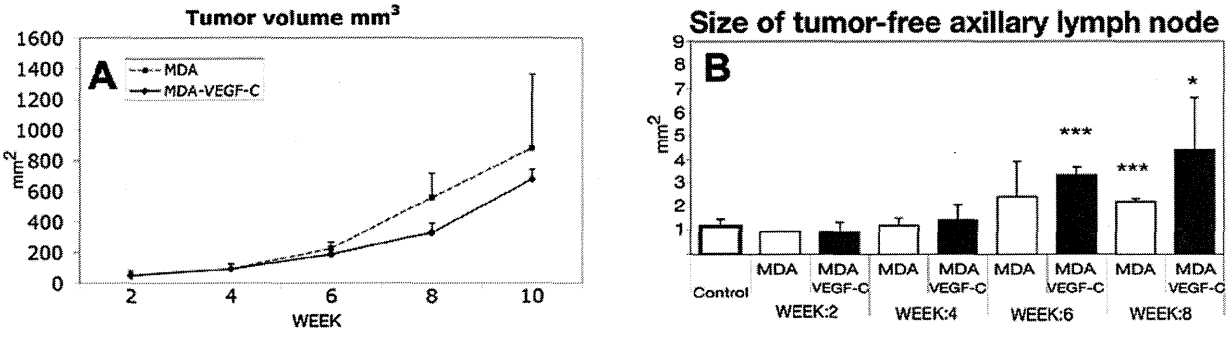

Figure 2. VEGF-C increases tumor-free sentinel lymph node size but not tumor volume. (A) No increase in the tumor growth rate (average size per mouse) of cancer formation was observed in VEGF-C dependency. Only at week 8 there was a significant increase of tumor volume of VEGF-C non-transfected MDA tumors. (B) Increased sentinel axillary lymph node size in mice bearing VEGF-C overexpressing tumors in comparison to control tumors and normal lymph nodes. Bars represent mean values ± SEM.

the control cell line (Fig. 2A). To determine if overexpression of VEGF-C leads to differences in sentinel lymph node size, we evaluated the tumor-free sentinel axillary lymph nodes every two weeks (Fig. 2B). The axillary lymph nodes were enlarged at the beginning of week 6, but until week 10 the size of the lymph nodes was not indicative of the presence of metastases. To obtain accurate quantitative analysis of metastases and lymph node involvement, we used cancer cells genetically labeled with GFP, a sensitive method for the direct visualization of micrometastases. Immunofluorescence for example revealed GFP expressing tumor cells entering the subcapsular sinus (Fig. 3A, arrow) from the tumor containing afferent lymphatic (Fig. 3A, arrowhead). To verify that tumor cells while *in vivo* did not lose their GFP vector every section was in addition evaluated by an H&E stain (Fig. 3B). Metastasis analysis, in agreement with our previously published data, revealed that the incidence of metastases was increased in VEGF-C- overexpressing tumors, as compared with the control tumors. The earliest metastasis in the VEGF-C overexpressing MDA cell line occurred at week 4, while in the control MDA cell line the first lymph node involvement was observed at week 8 (data not shown).

Lymph node lymphangiogenesis in sentinel lymph nodes. To investigate the effect of VEGF-C on the draining sentinel lymph node we determined differences of the lymphatic vessel area between the VEGF-C transfected and the control cell line. We evaluated the effect only on lymph nodes without presence of metastatic cells until week 4, an observation point with no visible and statistical difference in general tumor (Fig. 2A) and lymph node size (Fig. 2B). We found that the lymphatic vessel area in percent of the tumor-free lymph node was significantly increased in mice carrying VEGF-C-overexpressing tumors versus control tumors (Fig. 4A, $^{*}p<0.05$). We further observed no evidence of an increased blood vessel area in percent of the lymph node in mice carrying VEGF-C overexpressing tumors versus control tumors (Fig. 4B). Double-immunofluorescence staining revealed histological changes of the sentinel lymph nodes in mice carrying VEGF-C overexpressing tumors versus

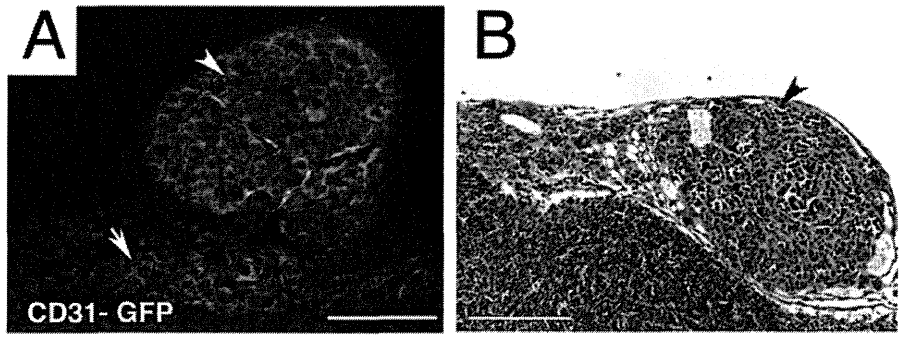

Figure 3. Involvement of draining lymphatics and lymphatic sinuses in sentinel lymph node metastasis. (A) GFP-expressing tumors and immunofluorescence staining for LYVE-1 (green)/CD31 (red) depicts involvement of lymph node lymphatic sinuses and blood vessels. Cell nuclei are stained with Hoechst (blue). Metastatic involvement was evaluated by fluorescence microscopy detecting (A) GFP expressing tumor cells and (B) by H&E, tumor cell dissemination in the subcapsular sinus (A, arrow) and in the afferent lymphatic vessel (A and B, arrowhead); scale bars, (A) 100 μm; (B) 200 μm.

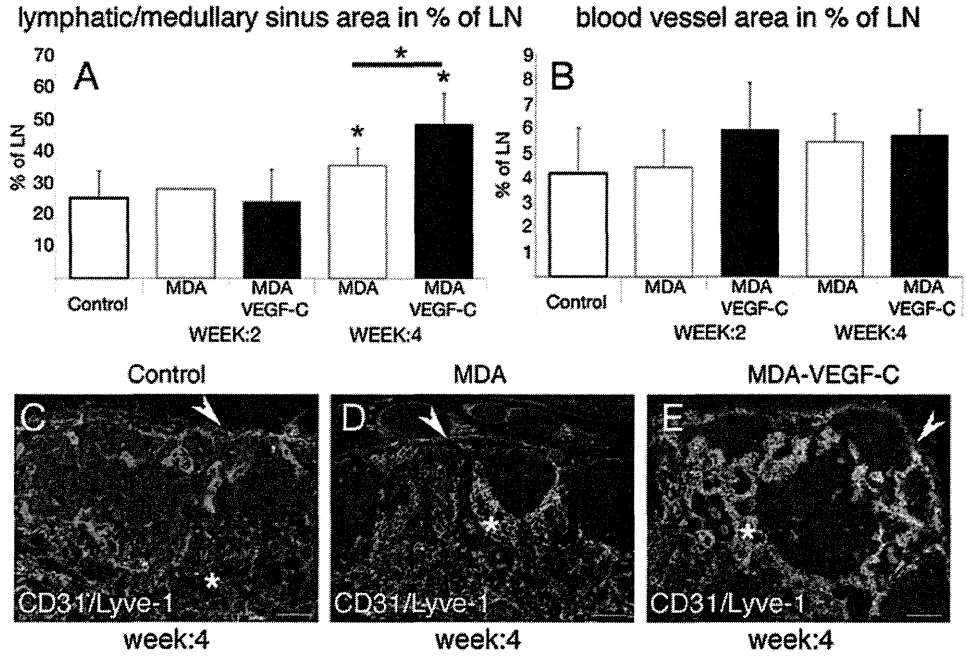

Figure 4. VEGF-C induces lymphatic sinus hyperplasia in sentinel lymph nodes. (A) Morphometric analysis revealed a significant increase of the lymphatic vessel area in sentinel lymph nodes draining VEGF-C overexpressing tumors as compared to the control tumor and normal lymph nodes. Sections were stained for LYVE-1 and CD31. Data are expressed as mean ± SD (*$p<0.05$). (B) Analysis revelaed no increase of the blood vessel area in sentinel lymph node draining VEGF-C overexpressing tumors as compared to the control tumor and normal lymph nodes. Sections were stained for LYVE-1 and CD31. Data are expressed as mean ± SD. (C-E) Immunofluorescence staining for LYVE-1 (green) and CD31 (red) depicts lymphatic vessel area and blood vessels in sentinel lymph nodes. (E) VEGF-C overexpressing tumors induce an increased area of the lymphatic sinuses network in sentinel lymph nodes as compared to the (D) control tumor and (C) normal lymph nodes; subcapsular sinus, arrowhead; *lymphatic sinuses; scale bar, 100 μm.

control tumors (Fig. 4C-E). In lymph nodes draining VEGF-C transfected tumors the profile of the lymphatic network had a globular appearance with an empty germinal center (Fig. 4C-E). These cup-shaped structures of the lymphatic sinuses (Fig. 4D and E) drained to the medullary sinuses just beneath the deep cortex (Fig. 4C-E). The number of follicles were not statistical different between the two groups (data not shown). In addition, we investigated if tumor associated macrophages revealed any difference in their recruitment, because VEGF-C might also have a direct impact on immune functions (8). VEGFR-3 was detected on macrophages *in vitro* and *in vivo*, and VEGF-C might induce an increased macrophage chemotaxis. To study this we stained the tumors for F4/80, an antigen that is expressed by a majority of mature macrophages. Immunofluorescence analyses revealed no difference in the infiltration of tumor-associated macrophages between the two groups (data not shown).

Discussion

Lymph nodes are the primary site of immune response and are a critical crossroad, since tumor cells, inflammatory and stroma cells could migrate towards and into them. Although morphological changes of lymph nodes involved and uninvolved in metastasis have been studied in various types of cancers, the

prognostic significance of immune response and lymph node size of tumor-free sentinel lymph nodes of breast carcinoma patients is unclear (15-17,31-37). This prompted us to investigate the early morphological changes of lymph vessels in sentinel lymph nodes in the premetastatic situation. In our model using VEGF-C transfected tumor cells versus control cells of the same cell line we observed that the lymph node size and tumor-associated immune response is not predictive for an subsequent metastasis. Both tumors, high- and low metastatic, induced equal lymph node size enlargement. Interestingly, our results suggest that LN-lymphangiogenesis in sentinel lymph nodes still uninvolved in metastasis could be a new early predictor of malignancy. LN-lymphangiogenesis induced by VEGF-C was revealed to be a very early morphological change in sentinel lymph nodes before overt metastasis. Previously, the function and role of VEGF-C was primarily investigated with regard to peritumoral and intratumoral tumor-lymphangiogenesis controlled by VEGFR-3 (5). VEGF-C, as the first lymphangiogenic factor, is proven to be expressed in various cancer cell types (reviewed in ref. 38) and it has been proven to play an active role in the interaction between tumors and lymphatics (1,3). It has been shown that the induction of lymphangiogenesis is a prognostic indicator of the metastatic risk of malignant melanoma of the skin (4), but only a few studies have investigated the effect of tumor derived lymphangiogenic factors on sentinel lymph nodes (6,10-12). We found in a carcinogenesis model that transgenic overexpression of VEGF-A and VEGF-C in the skin induced sentinel lymph node lymphangiogenesis (10,11), also when released by chronically inflamed tissue (39). Our study reported here demonstrates that cancer derived VEGF-C induces sentinel lymph node lymphatic hyperplasia without altering the blood vessel area and lymph node size. Transgenic overexpression of VEGF-C at early time points resulted in an increased lymphatic hyperplasia in VEGF-C draining sentinel lymph nodes in comparison to the control tumors not overexpressing VEGF-C even before the tumor had metastasized.

Based on this observation it could be hypothesized that LN-lymphangiogenesis facilitates tumor cell metastasis, an early event of distant organ metastasis. Hirakawa *et al* recently observed this in VEGF-C overexpressing skin tumors (10), but the role of LN-lymphangiogenesis and its inhibition in the further dissemination of cancer remains largely unexplored. In clinical oncology the size of sentinel lymph nodes has emerged as a predictor next to the extracapsular growth, size of the primary tumor and prescence of lymphovascular invasion, as reported by Van Zee *et al* (40). It has been observed that LN-lymphangiogenesis was associated with an increased frequency of involved non-sentinel lymph nodes in humans (41). The findings suggest that primary tumors, via secretion of lymphangiogenic factors such as VEGF-C induce lymphatic sinus hyperplasia of the sentinel lymph node and thereby might promote their further spread. Recent evidence even indicated that LN-lymphangiogenesis increased lymph flow actively about 20- to 30-fold (6). Although overexpression of VEGF-C induced a more pronounced lymphatic network of sentinel lymph nodes, also the control MDA cell line induced LN-lymphangiogenesis, which indicates that there must be different mechanisms in addition to VEGF-C release. Inflammatory reactions due to tumor necrosis have already been postulated to have an effect on lymph node hyperplasia (42). Especially for inflammatory breast cancers it has been described that they have an angiogenic phenotype and that factors such VEGF-C, VEGF-D and FGF-2 are increased in comparison to non-inflammatory breast carcinomas (43-45). In our xenograft model lymphangiogenic factors produced by macrophages could be a possible explanation, due to the fact that tumor associated macrophages have been identified to produce a broad variety of lymphangiogenic and angiogenic factors (46). We determined the difference of tumor-associated macrophages to exclude that VEGF-C induced a more pronounced secondary response by inducing an increased macrophage chemotaxis, acting via the VEGF-receptor 3 expressed by macrophages (8,46). We found no difference in macrophage infiltration pattern. Studies in which VEGF-A, VEGF-C, FGF-2 or other growth factors in this setting are blocked might answer the question of relative importance of one or more of these factors alone or in concert and could be important for further cancer treatment approaches.

Importantly, our study reveals that the lymphatic network of sentinel lymph nodes should be specifically evaluated by using specific lymphatic endothelial markers. In agreement with the previously published finding by Hattori (47), we recommend that the evaluation of lymph node vessels should not be done by a PECAM-1 (CD31) staining. CD31 is also expressed on the lymphatic sinus network endothelium, but cannot distinguish between the lymphatic and blood vascular system.

Our findings provide additional data to the previously proposed 'seed and soil hypothesis' (11), inasmuch as primary tumors might prepare their future metastatic site by producing lymphangiogenic factors that support efficient transport to sentinel lymph nodes, distant lymph nodes and organ sites.

Early changes of the lymphatic sinuses and lymphangiogenesis might predict an unfavorable outcome of an individual carcinoma patient. The lymphatic sinus network of sentinel lymph nodes could even be an important target for future therapies.

Acknowledgements

We thank M. Constant, L. Janes and L. Nguyen for expert technical assistance. This work was supported by NIH grants CA69184, CA86410, CA92644 (MD), American Cancer Society Research Project Grant 99-23901 (MD), Swiss National Fund grant 3100A0-108207 (MD), Fonds für wissenschaftliche Förderung grant S9408-B11 (MD), and by the Deutsche Krebshilfe (RL).

References

1. Skobe M, Hawighorst T, Jackson DG, *et al*: Induction of tumor lymphangiogenesis by VEGF-C promotes breast cancer metastasis. Nat Med 7: 192-198, 2001.
2. Stacker SA, Caesar C, Baldwin ME, *et al*: VEGF-D promotes the metastatic spread of tumor cells via the lymphatics. Nat Med 7: 186-191, 2001.
3. Mandriota SJ, Jussila L, Jeltsch M, *et al*: Vascular endothelial growth factor-C-mediated lymphangiogenesis promotes tumour metastasis. EMBO J 20: 672-682, 2001.
4. Dadras SS, Paul T, Bertoncini J, *et al*: Tumor lymphangiogenesis: a novel prognostic indicator for cutaneous melanoma metastasis and survival. Am J Pathol 162: 1951-1960, 2003.
5. Jussila L and Alitalo K: Vascular growth factors and lymphangiogenesis. Physiol Rev 82: 673-700, 2002.

6. Ruddell A, Mezquita P, Brandvold KA, Farr A and Iritani BM: B lymphocyte-specific c-Myc expression stimulates early and functional expansion of the vasculature and lymphatics during lymphomagenesis. Am J Pathol 163: 2233-2245, 2003.
7. Mattila MM, Ruohola JK, Karpanen T, Jackson DG, Alitalo K and Harkonen PL: VEGF-C induced lymphangiogenesis is associated with lymph node metastasis in orthotopic MCF-7 tumors. Int J Cancer 98: 946-951, 2002.
8. Skobe M, Hamberg LM, Hawighorst T, *et al*: Concurrent induction of lymphangiogenesis, angiogenesis, and macrophage recruitment by vascular endothelial growth factor-C in melanoma. Am J Pathol 159: 893-903, 2001.
9. Karpanen T, Egeblad M, Karkkainen MJ, *et al*: Vascular endothelial growth factor C promotes tumor lymphangiogenesis and intralymphatic tumor growth. Cancer Res 61: 1786-1790, 2001.
10. Hirakawa S, Brown LF, Kodama S, Paavonen K, Alitalo K and Detmar M: VEGF-C-induced lymphangiogenesis in sentinel lymph nodes promotes tumor metastasis to distant sites. Blood 109: 1010-1017, 2007.
11. Hirakawa S, Kodama S, Kunstfeld R, Kajiya K, Brown LF and Detmar M: VEGF-A induces tumor and sentinel lymph node lymphangiogenesis and promotes lymphatic metastasis. J Exp Med 201: 1089-1099, 2005.
12. Harrell MI, Iritani BM and Ruddell A: Tumor-induced sentinel lymph node lymphangiogenesis and increased lymph flow precede melanoma metastasis. Am J Pathol 170: 774-786, 2007.
13. McGuire WL and Clark GM: Prognostic factors and treatment decisions in axillary-node-negative breast cancer. N Engl J Med 326: 1756-1761, 1992.
14. Shuster TD, Girshovich L, Whitney TM and Hughes KS: Multidisciplinary care for patients with breast cancer. Surg Clin North Am 80: 505-533, 2000.
15. Salama JK, Heimann R, Lin F, *et al*: Does the number of lymph nodes examined in patients with lymph node-negative breast carcinoma have prognostic significance? Cancer 103: 664-671, 2005.
16. Moorman PG, Hamza A, Marks JR and Olson JA: Prognostic significance of the number of lymph nodes examined in patients with lymph node-negative breast carcinoma. Cancer 91: 2258-2262, 2001.
17. Camp RL, Rimm EB and Rimm DL: A high number of tumor free axillary lymph nodes from patients with lymph node negative breast carcinoma is associated with poor outcome. Cancer 88: 108-113, 2000.
18. Okada S, Albrecht RM, Aharinejad S and Schraufnagel DE: Structural aspects of the lymphocyte traffic in rat submandibular lymph node. Microsc Microanal 8: 116-133, 2002.
19. Hall JG and Morris B: The origin of the cells in the efferent lymph from a single lymph node. J Exp Med 121: 901-910, 1965.
20. Cahill RN, Frost H and Trnka Z: The effects of antigen on the migration of recirculating lymphocytes through single lymph nodes. J Exp Med 143: 870-888, 1976.
21. Lacroix M: MDA-MB-435 cells are from melanoma, not from breast cancer. Cancer Chemother Pharmacol 63: 567, 2009.
22. Ross DT, Scherf U, Eisen MB, *et al*: Systematic variation in gene expression patterns in human cancer cell lines. Nat Genet 24: 227-235, 2000.
23. Joukov V, Pajusola K, Kaipainen A, *et al*: A novel vascular endothelial growth factor, VEGF-C, is a ligand for the Flt4 (VEGFR-3) and KDR (VEGFR-2) receptor tyrosine kinases. EMBO J 15: 1751, 1996.
24. Sato Y, Mukai K, Watanabe S, Goto M and Shimosato Y: The AMeX method. A simplified technique of tissue processing and paraffin embedding with improved preservation of antigens for immunostaining. Am J Pathol 125: 431-435, 1986.
25. Streit M, Stephen AE, Hawighorst T, *et al*: Systemic inhibition of tumor growth and angiogenesis by thrombospondin-2 using cell-based antiangiogenic gene therapy. Cancer Res 62: 2004-2012, 2002.
26. Hong YK, Shin JW and Detmar M: Development of the lymphatic vascular system: a mystery unravels. Dev Dyn 231: 462-473, 2004.
27. He Y: Scanning electron microscope studies of the rat mesenteric lymph node with special reference to high-endothelial venules and hitherto unknown lymphatic labyrinth. Arch Histol Jpn 48: 1-15, 1985.
28. Ohtani O, Ohtani Y, Carati CJ and Gannon BJ: Fluid and cellular pathways of rat lymph nodes in relation to lymphatic labyrinths and Aquaporin-1 expression. Arch Histol Cytol 66: 261-272, 2003.
29. Belz GT and Heath TJ: Lymph pathways of the medial retropharyngeal lymph node in dogs. J Anat 186: 517-526, 1995.
30. Nicander L, Nafstad P, Landsverk T and Engebretsen RH: A study of modified lymphatics in the deep cortex of ruminant lymph nodes. J Anat 178: 203-212, 1991.
31. Black MM and Zachrau RE: Antitumor immunity in breast cancer patients. Biologic and therapeutic implications. J Reprod Med 23: 21-32, 1979.
32. Tsakraklides V, Anastassiades OT and Kersey JH: Prognostic significance of regional lymph node histology in uterine cervical cancer. Cancer 31: 860-868, 1973.
33. Tsakraklides V, Olson P, Kersey JH and Good RA: Prognostic significance of the regional lymph node histology in cancer of the breast. Cancer 34: 1259-1267, 1974.
34. Oka M, Yoshino S, Hazama S, Shimoda K, Suzuki M and Suzuki T: Prognostic significance of regional lymph node reaction after curative resection of advanced gastric cancer. Br J Surg 79: 1091-1094, 1992.
35. Black MM, Freeman C, Mork T, Harvei S and Cutler SJ: Prognostic significance of microscopic structure of gastric carcinomas and their regional lymph nodes. Cancer 27: 703-711, 1971.
36. Bennett SH, Futrell JW, Roth JA, Hoye RC and Ketcham AS: Prognostic significance of histologic host response in cancer of the larynx or hypopharynx. Cancer 28: 1255-1265, 1971.
37. Malicka K: Attempt at evaluation of defensive activity of lymph nodes on the basis of microscopic and clinical studies in cases of laryngeal cancer. Pol Med J 10: 154-164, 1971.
38. Cassella M and Skobe M: Lymphatic vessel activation in cancer. Ann NY Acad Sci 979: 120-130, 2002.
39. Halin C, Tobler NE, Vigl B, Brown LF and Detmar M: VEGF-A produced by chronically inflamed tissue induces lymphangiogenesis in draining lymph nodes. Blood 110: 3158-3167, 2007.
40. Van Zee KJ, Manasseh DM, Bevilacqua JL, *et al*: A nomogram for predicting the likelihood of additional nodal metastases in breast cancer patients with a positive sentinel node biopsy. Ann Surg Oncol 10: 1140-1151, 2003.
41. Van den Eynden GG, Vandenberghe MK, van Dam PJ, *et al*: Increased sentinel lymph node lymphangiogenesis is associated with nonsentinel axillary lymph node involvement in breast cancer patients with a positive sentinel node. Clin Cancer Res 13: 5391-5397, 2007.
42. Studer UE, Scherz S, Scheidegger J, *et al*: Enlargement of regional lymph nodes in renal cell carcinoma is often not due to metastases. J Urol 144: 243-245, 1990.
43. Van der Auwera I, Van Laere SJ, Van den Eynden GG, *et al*: Increased angiogenesis and lymphangiogenesis in inflammatory versus noninflammatory breast cancer by real-time reverse transcriptase-PCR gene expression quantification. Clin Cancer Res 10: 7965-7971, 2004.
44. Shirakawa K, Shibuya M, Heike Y, *et al*: Tumor-infiltrating endothelial cells and endothelial precursor cells in inflammatory breast cancer. Int J Cancer 99: 344-351, 2002.
45. Padera TP, Kadambi A, di Tomaso E, *et al*: Lymphatic metastasis in the absence of functional intratumor lymphatics. Science 296: 1883-1886, 2002.
46. Schoppmann SF, Birner P, Stockl J, *et al*: Tumor-associated macrophages express lymphatic endothelial growth factors and are related to peritumoral lymphangiogenesis. Am J Pathol 161: 947-956, 2002.
47. Hattori H: Caution should be taken in using CD31 for distinguishing the vasculature of lymph nodes. J Clin Pathol 56: 638-639, 2003.

The American Journal of Pathology, Vol. 181, No. 6, December 2012

http://dx.doi.org/10.1016/j.ajpath.2012.08.023

Vascular Biology, Atherosclerosis, and Endothelium Biology

Topical Simvastatin Accelerates Wound Healing in Diabetes by Enhancing Angiogenesis and Lymphangiogenesis

Jun Asai,* Hideya Takenaka,* Satoshi Hirakawa,† Jun-ichi Sakabe,† Asami Hagura,* Saburo Kishimoto,* Kazuichi Maruyama,‡ Kentaro Kajiya,§ Shigeru Kinoshita,‡ Yoshiki Tokura,† and Norito Katoh*

From the Departments of Dermatology and Ophthalmology,‡ Graduate School of Medical Science, Kyoto Prefectural University of Medicine, Kyoto; the Department of Dermatology,† Hamamatsu University School of Medicine, Hamamatsu; and the Shiseido Innovative Science Research Center,§ Yokohama, Japan*

Impaired wound healing is a major complication of diabetes. Recent studies have reported reduced lymphangiogenesis and angiogenesis during diabetic wound healing, which are thought to be new therapeutic targets. Statins have effects beyond cholesterol reduction and can stimulate angiogenesis when used systemically. However, the effects of topically applied statins on wound healing have not been well investigated. The present study tested the hypothesis that topical application of simvastatin would promote lymphangiogenesis and angiogenesis during wound healing in genetically diabetic mice. A full-thickness skin wound was generated on the back of the diabetic mice and treated with simvastatin or vehicle topically. Simvastatin administration resulted in significant acceleration of wound recovery, which was notable for increases in both angiogenesis and lymphangiogenesis. Furthermore, simvastatin promoted infiltration of macrophages, which produced vascular endothelial growth factor C in granulation tissues. *In vitro*, simvastatin directly promoted capillary morphogenesis and exerted an antiapoptotic effect on lymphatic endothelial cells. These results suggest that the favorable effects of simvastatin on lymphangiogenesis are due to both a direct influence on lymphatics and indirect effects via macrophages homing to the wound. In conclusion, a simple strategy of topically applied simvastatin may have significant therapeutic potential for enhanced wound healing in patients with impaired microcirculation such as that in diabetes. *(Am J Pathol 2012, 181:2217–2224; http://dx.doi.org/10.1016/j.ajpath.2012.08.023)*

Delayed wound healing is a major complication of diabetes and is caused by increased apoptosis, delayed cellular infiltration, reduced angiogenesis, and decreased formation and organization of collagen fibers.[1–3] Impaired lymphangiogenesis has also recently been established as a major factor in diabetic refractory wound healing.[4,5] The functions of lymphatic vessels in wounds are to drain the protein-rich lymph from the extracellular space, to maintain normal tissue pressure, and to mediate the immune response.[6,7] Delayed wound healing, such as that seen in infections, appears to result from persistent edema and delayed removal of debris and inflammatory cells due to reduced lymphatic development.[8]

Statins are HMG-CoA (5-hydroxy-3-methylglutaryl-coenzyme A) reductase inhibitors that are primarily used to lower circulating cholesterol levels. In addition, statins have been found to protect against ischemic injury and stimulate angiogenesis in normocholesterolemic animals.[9–11] This angiogenic effect is partially mediated by direct regulation of proliferation of endothelial cells and capillary morphogenesis via the Akt/PI3K pathway.[11] Simvastatin has been found to enhance vascular endothelial growth factor (VEGF) production and improve wound healing in an experimental model of diabetes,[12] and nitropravastatin stimulates reparative neovascularization and improves recovery from limb ischemia in type 1 diabetic mice.[13] However, systemic administration at an extremely high dose was used to obtain angiogenic effects in

Supported by grants from the Ministry of Education, Culture, Sports, Science and Technology of Japan.

Accepted for publication August 15, 2012.

CME Disclosure: The authors of this article and the planning committee members and staff have no relevant financial relationships with commercial interest to disclose.

Supplemental material for this article can be found at *http://ajp.amjapathol.org* or at *http://dx.doi.org/10.1016/j.ajpath.2012.08.023*.

Address reprint requests to Jun Asai, M.D., Ph.D., Department of Dermatology, Graduate School of Medical Science, Kyoto Prefectural University of Medicine, 465 Hirokoji, Kawaramachi, Kamigyo-Ku, Kyoto, 602-8566, Japan. E-mail: jasai@koto.kpu-m.ac.jp.

these studies, and this is inapplicable for clinical use as an angiogenic drug in patients with ischemic disorders. However, topical application of statins with avoidance of systemic adverse effects may be useful for cutaneous wound healing, in which angiogenesis plays a pivotal role.[14] The lymphangiogenic effects of statins have not been widely investigated. In this study, we evaluated the effects of topical simvastatin on angiogenesis and lymphangiogenesis in a mouse model of impaired diabetic wound healing.

Materials and Methods

Animals

Genetically diabetic C57BLKS/J-m+/+*Lepr*^{db} mice (db/db mice) were obtained from Clea Japan, Inc. (Tokyo, Japan). All procedures were performed in accordance with the guidelines of the Animal Care and Use Committees of Kyoto Prefectural University of Medicine.

Creation of Wounds

Mice were between 6 and 10 weeks old at the time of the study. Wounds were generated as described previously.[15–17] In brief, after induction of deep anesthesia by i.p. injection of sodium pentobarbital (160 mg/kg), full-thickness, excisional skin wounds using 8-mm skin biopsy punches were made on the backs of mice, with one wound generated in each mouse. Each wound was covered with a semipermeable polyurethane dressing (OpSite; Smith and Nephew, Massillon, OH) after topical application of simvastatin (Calbiochem, La Jolla, CA) in petroleum jelly (a mixture of 5 mg of simvastatin and 995 mg of jelly) or vehicle (petroleum jelly alone). Simvastatin in petroleum jelly (10 mg of the mixture containing 50 μg of simvastatin) or vehicle were applied to the wound on days 0, 4, 7, and 10 after creation of the wound.

Monitoring of Wound Healing

A total of 5 db/db mice were used at each time point. Wound healing was monitored by taking pictures with a digital camera (Nikon Coolpix 995; Nikon, Tokyo, Japan) on days 0, 4, 7, and 14 after wound creation. Images were analyzed using ImageJ software version 1.46 (NIH, Bethesda, MD)[18] by tracing the wound margin with a high-resolution computer mouse and calculating the pixel area. Wound closure was calculated as follows: Percentage Closed = [(Area on Day 0 − Open Area on Final Day)/Area on Day 0] × 100, as described previously.[15] The areas of the wounds were compared with Student's *t*-test with $P < 0.05$ taken to indicate a significant difference.

Histologic Score

A histologic score was assigned in a masked manner as described previously.[15] Briefly, each specimen received a score of 1 to 12 as follows: 1 to 3, none to minimal cell accumulation and granulation tissue or epithelial migration; 4 to 6, thin, immature granulation dominated by inflammatory cells but with few fibroblasts, capillaries, or collagen deposition and minimal epithelial migration; 7 to 9, moderately thick granulation tissue, ranging from mainly inflammatory cells to more fibroblasts and collagen deposition; and 10 to 12, thick, vascular granulation tissue dominated by fibroblasts and extensive collagen deposition.

Evaluation of Wound Angiogenesis and Lymphangiogenesis

Sections were stained with rat anti-CD31 antibody (1:100) (BD Biosciences, San Jose, CA) or rabbit anti-LYVE-1 antibody (Upstate, Lake Placid, NY). Green fluorescence was generated by labeling with fluorescein isothiocyanate (FITC)–streptavidin (Vector Laboratories, Burlingame, CA) and biotinylated anti-rat or anti-rabbit antibody (both Vector Laboratories). Wound angiogenesis or lymphangiogenesis was analyzed by calculating the percentage of fluorescent area.[16,19] Briefly, for each slide, an image of the granulation tissue at the wound margin was captured. ImageJ software was used to quantitate the fluorescence intensity. The mean percentage of fluorescent pixels of five images served as an index of the angiogenic or lymphangiogenic response.

Evaluation of Macrophage Number, Phenotype, and VEGF-C Expression in Granulation Tissue

Sections of wounds were stained with rat anti-F4/80 antibody (Invitrogen, Carlsbad, CA). Labeling with F4/80 was visualized with Cy3-conjugated anti-rat antibody (Vector Laboratories). Ten granulation tissue fields (two sections from each animal) were selected, and F4/80-positive cells were counted.[16] VEGF-C expression was evaluated using goat anti-VEGF-C antibody (Santa Cruz Biotechnology, Santa Cruz, CA) and FITC-conjugated anti-goat antibody (Vector Laboratories). To determine the phenotype of infiltrating macrophages, IL-13 and tumor necrosis factor (TNF) α expression was evaluated using goat anti-IL-13 antibody and goat anti-TNF-α antibody (Santa Cruz Biotechnology), respectively, and FITC-conjugated anti-goat antibody. F4/80-positive TNF-α–positive cells were defined as an M1 phenotype and F4/80-positive IL-13–positive cells as an M2 phenotype. In each slide, F4/80-positive cells, F4/80-positive TNF-α–positive cells, and F4/80-positive IL-13–positive cells were counted, and percentages of TNF-α–positive macrophages and IL-13–positive macrophages were evaluated. The mean percentages of TNF-α–positive macrophages and IL-13–positive macrophages in five images were used as indexes of the M1 and M2 phenotypes, respectively.

RNA Isolation, cDNA Synthesis, and Quantitative RT-PCR

Tissue sections obtained in RNAlater (Ambion, Paisley, UK) were processed for RNA isolation, cDNA synthesis, and quantitative RT-PCR.[16] VEGF-C, fibroblast growth factor 2, endothelial nitric oxide synthase, stromal cell-derived factor 1α, and platelet-derived growth factor β gene expression levels were normalized based on the level of an internal

reference gene, 18S. The primers used in the study were obtained from QIAGEN (Düsseldorf, Germany).

Cell Culture

Primary human lymphatic endothelial cells (LECs) were collected as previously described.[20] LECs were cultured at 37°C in 5% CO_2 in endothelial cell basal medium 2 (Lonza, Walkersville, MD) supplemented with 5% fetal bovine serum, human VEGF-A, human fibroblast growth factor 2, human epidermal growth factor, insulin-like growth factor 1, and ascorbic acid. Each experiment was conducted at least three times, with similar results. A representative experiment is shown.

Western Blot Analysis

Cells were lysed with RIPA buffer (Invitrogen) and sonicated. After sonication, cell lysates were centrifuged at 15,400 × *g* for 20 minutes at 4°C, and the supernatants were collected into fresh tubes. Then 4× SDS sample buffer with 0.1 mol/L dithiothreitol was added to samples. Samples were boiled for 5 minutes at 95°C, and 20-μg extracts were separated by 10% SDS-PAGE and electroblotted onto polyvinylidene difluoride membranes for 2 hours at 180 mA. The membranes were incubated with rabbit anti-human Akt (pan) (C67E7) monoclonal antibody (Cell Signaling Technology, Danvers, MA), rabbit anti-human phospho-Akt (Ser473) (D9E) monoclonal antibody (Cell Signaling Technology), or mouse anti-GAPDH monoclonal antibody (Santa Cruz Biotechnology) and detected with horseradish peroxidase–conjugated goat anti-rabbit IgG (Bio-Rad, Hercules, CA) or horseradish peroxidase–conjugated goat anti-mouse IgG (Bio-Rad). Immunoblots were visualized using an ECL Plus Western Blotting Detection Reagents Kit (GE Healthcare, Little Chalfont, Buckinghamshire, UK) according to the manufacturer protocol.

Chord Formation Assay

LECs were used in a chord formation assay.[21] An aliquot (100 μL) of growth factor–depleted Matrigel (Becton Dickinson, Bedford, MA) was added to a 24-well dish and allowed to gel for 30 minutes at 37°C. LECs were seeded at 5×10^4 cells/mL in 500 μL of endothelial cell basal medium 2 containing 3% fetal bovine serum. Cells were cultured in the absence or presence of various doses of simvastatin (Calbiochem, Darmstadt, Germany) with or without pretreatment with a PI3 kinase inhibitor, LY294002 (50 μmol/L) (ENZO Life Sciences, Plymouth Meeting, PA), the mTOR/raptor inhibitor rapamycin (100 nmol/L) (Merck Millipore, Darmstadt, Germany), or the PI3K/mTOR inhibitor wortmannin-rapamycin (100 nmol/L) (Cayman Chemical, Ann Arbor, MI) for 30 minutes. Chord formation was monitored for 24 hours. Digital pictures were taken using a spot image analysis system, and the total length of the chord-like structures at 12 hours was outlined and measured using ImageJ software.

Proliferation Assay

The proliferative activity of cells treated with simvastatin was examined using a CellTiter 96 nonradioactive cell proliferation assay (Promega, Madison, WI). Briefly, subconfluent cells (5000 cells per well) were reseeded on 96-well, flat-bottomed plates with 100 μL of growth media. The cells were treated with simvastatin and incubated for 48 hours at 37°C. Absorbance at 570 nm was recorded using a 96-well enzyme-linked immunosorbent assay (ELISA) plate reader.

Apoptosis Assay

An apoptosis assay was performed using a DeadEnd Fluorometric TUNEL System (Promega). Briefly, LECs were plated on chamber slides and placed in medium. Cells were stimulated by simvastatin and incubated for 24 hours with medium containing 400 μmol/L H_2O_2. To quantify apoptosis, 400 nuclei from random microscopic fields were analyzed by an observer masked to the treatment groups. The number of apoptotic cells was expressed as a percentage of the total cell count.

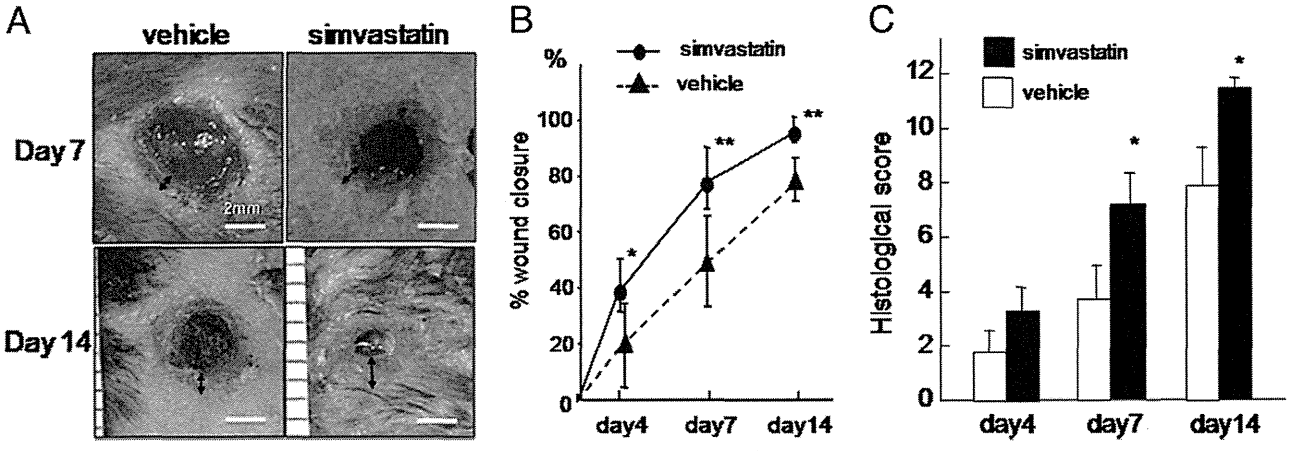

Figure 1. Effects of topical simvastatin on wound closure and histologic score in db/db mice. **A:** Representative macroscopic views of wounds after different treatments and periods. Scale bar = 2 mm. **Arrows** indicate the epithelialized range. **B:** Wound closure was measured on days 4, 7, and 14. $^*P < 0.05$, $^{**}P < 0.001$ versus vehicle ($n = 5$ in each group). **C:** Histologic scores for days 4, 7, and 14, quantified as described in *Materials and Methods*. Higher histologic scores indicate a greater extent of wound healing. $^*P < 0.05$ versus vehicle ($n = 5$ in each group).

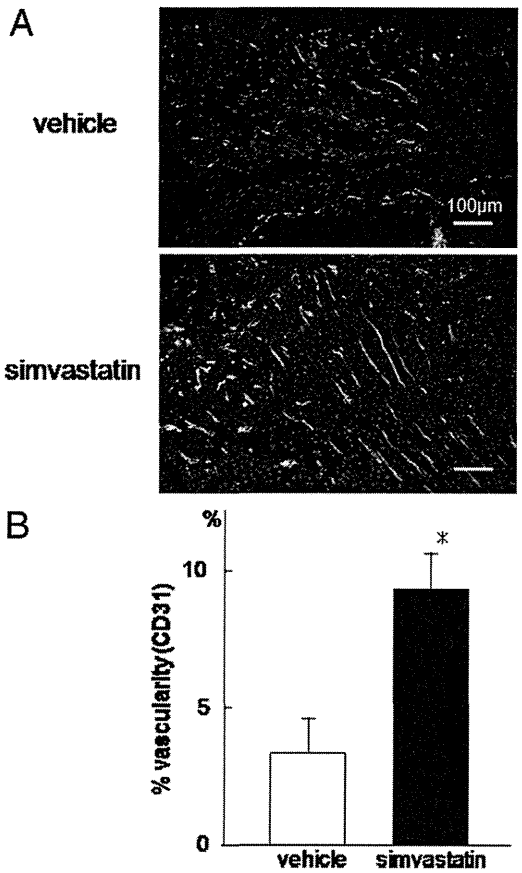

Figure 2. Effects of simvastatin on vascularity in granulation tissues at the wound margin in db/db mice. **A:** Neovascularization at the wound margin in simvastatin- or vehicle-treated diabetic mice after 14 days. Original magnification, ×100. Scale bar = 100 μm. Green and blue fluorescence corresponds to CD31-positive newly formed blood vessels and DAPI-labeled nuclei, respectively. **B:** Percentage of vascularity, quantified as described in *Materials and Methods*. *$P < 0.001$ versus vehicle ($n = 5$ in each group).

Statistical Analysis

All results are presented as mean ± SEM. Statistical comparisons between two groups were performed by Student's *t*-test. Multiple groups were analyzed by one-way analysis of variance followed by appropriate post hoc tests to determine statistical significance. $P < 0.05$ was considered significant. All *in vitro* experiments were performed at least in triplicate.

Results

Simvastatin Accelerates Wound Healing in Diabetic Mice

Wound areas on days 7 and 14 in simvastatin- or vehicle-treated diabetic mice are shown in Figure 1A. On day 14, simvastatin-treated wounds had more than 90% epithelialization, whereas <80% of the wound was epithelialized in the vehicle-treated group (Figure 1B). Simvastatin treatment resulted in significantly smaller wound areas after 4, 7, and 14 days. The difference in percentage of wound closure reached a maximum on day 7 (simvastatin versus control: 79.26% ± 11.09% versus 52.45% ± 16.81%; $P < 0.001$). The histologic score reflects the degree of maturation of granulation tissue, including inflammation, collagen deposition, and reepithelialization, in addition to neovascularization; therefore, higher histologic scores reflect a greater extent of wound healing. The histologic scores for wounds treated with simvastatin were significantly higher than those in the vehicle-treated group (day 4: 3.6 ± 0.70 versus 1.9 ± 0.73; day 7: 7.3 ± 0.94 versus 3.7 ± 0.94, $P < 0.01$; day 14: 11.6 ± 0.51 versus 8.0 ± 1.15, $P < 0.01$)(Figure 1C).

Simvastatin Promotes Both Angiogenesis and Lymphangiogenesis

Wound angiogenesis was analyzed by immunostaining of an endothelial cell–specific marker, CD31, in 10-μm frozen sections to visualize neovascularization. Figure 2A shows neovascularization at the margin in simvastatin- or vehicle-treated wounds in diabetic mice on day 14. A few small vessels were seen at the wound margin in the vehicle-treated group, whereas large numbers of vessels were growing toward the center of the wound in the

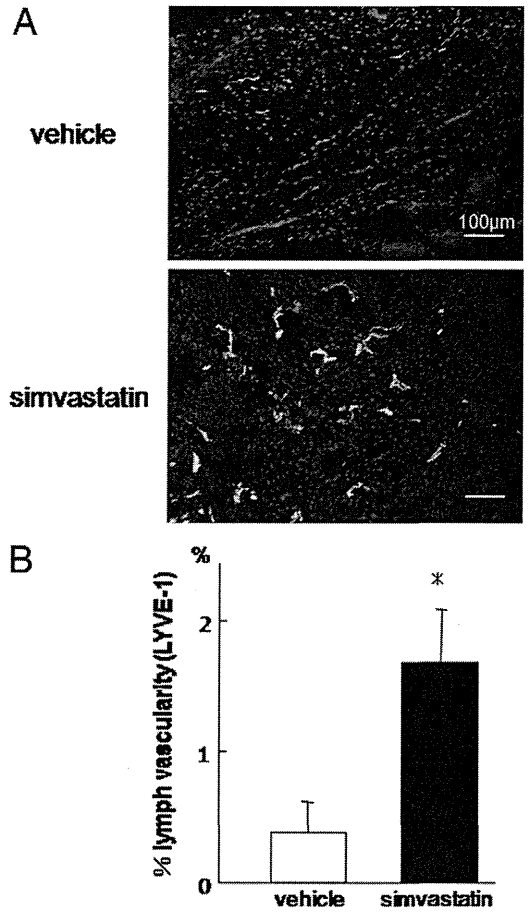

Figure 3. Effects of simvastatin on lymphangiogenesis in granulation tissues at the wound margin in db/db mice. **A:** Lymphangiogenesis at the wound margin in simvastatin- or vehicle-treated diabetic mice after 14 days. Original magnification, ×100. Scale bar =100 μm. Green and blue fluorescence corresponds to LYVE-1–positive newly formed lymphatic vessels and DAPI-labeled nuclei, respectively. **B:** Percentage of lymphatic vascularity, quantified as described in *Materials and Methods*. *$P < 0.001$ versus vehicle ($n = 5$ in each group).

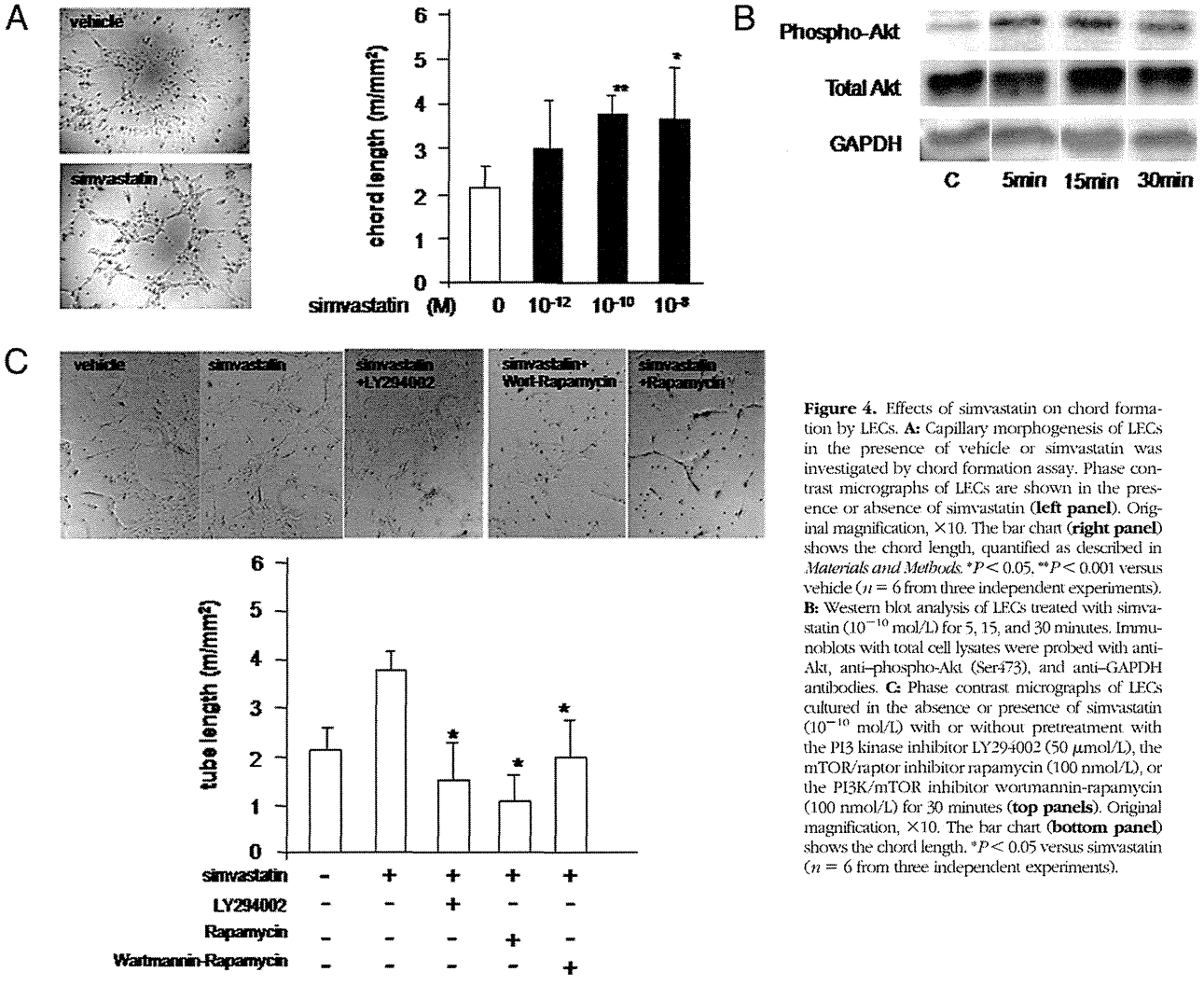

Figure 4. Effects of simvastatin on chord formation by LECs. **A:** Capillary morphogenesis of LECs in the presence of vehicle or simvastatin was investigated by chord formation assay. Phase contrast micrographs of LECs are shown in the presence or absence of simvastatin (**left panel**). Original magnification, ×10. The bar chart (**right panel**) shows the chord length, quantified as described in *Materials and Methods*. $^{*}P < 0.05$, $^{**}P < 0.001$ versus vehicle ($n = 6$ from three independent experiments). **B:** Western blot analysis of LECs treated with simvastatin (10^{-10} mol/L) for 5, 15, and 30 minutes. Immunoblots with total cell lysates were probed with anti-Akt, anti–phospho-Akt (Ser473), and anti-GAPDH antibodies. **C:** Phase contrast micrographs of LECs cultured in the absence or presence of simvastatin (10^{-10} mol/L) with or without pretreatment with the PI3 kinase inhibitor LY294002 (50 μmol/L), the mTOR/raptor inhibitor rapamycin (100 nmol/L), or the PI3K/mTOR inhibitor wortmannin-rapamycin (100 nmol/L) for 30 minutes (**top panels**). Original magnification, ×10. The bar chart (**bottom panel**) shows the chord length. $^{*}P < 0.05$ versus simvastatin ($n = 6$ from three independent experiments).

simvastatin group. Simvastatin significantly enhanced wound vascularity based on image analysis of the percentage of the fluorescent area (9.29% ± 1.29% versus 3.25% ± 1.33%; $P < 0.001$)(Figure 2B). Wound lymphangiogenesis was analyzed by immunostaining of a LEC-specific marker, LYVE-1, in 10-μm frozen sections. Figure 3A shows new lymphatic vessels at the margin of simvastatin- or vehicle-treated wounds in diabetic mice on day 14. Wound lymphatic vascularity was significantly enhanced by simvastatin (percentage of fluorescent area: 1.72% ± 0.460% versus 0.395% ± 0.260%; $P < 0.001$) (Figure 3B). New vessels and lymphatics in granulation tissue in both groups were not covered with α-smooth muscle actin–positive mural cells (see Supplemental Figure S1 at *http://ajp.amjpathol.org*).

Simvastatin Induces Capillary Morphogenesis of LECs and Has an Antiapoptotic Effect but Does Not Induce Proliferation

To characterize the effects of simvastatin on lymphangiogenesis, we performed a chord formation assay in primary human LECs *in vitro*. Treatment with simvastatin promoted LEC chord formation in a dose-dependent manner (Figure 4A). This effect was significantly blocked by the PI3 kinase inhibitor LY294002, the mTOR inhibitor rapamycin, and the PI3/mTOR inhibitor wortmannin-rapamycin ($P < 0.05$)(Figure 4C). The proliferative and antiapoptotic effects of simvastatin on LECs were also examined because these are major effects of simvastatin in vascular endothelial cells. Simvastatin did not promote LEC proliferation, even at higher concentrations, and seemed to be slightly cytotoxic at 10^{-6} mol/L and 10^{-5} mol/L (Figure 5A). However, simvastatin treatment resulted in significant inhibition of H_2O_2-induced apoptosis compared with controls (Figure 5B).

Simvastatin Promotes Macrophage Infiltration and VEGF-C Production in Wounds

The number of macrophages in granulation tissues was evaluated in wounds on day 7. This timing was chosen because reepithelialization was almost complete on day 14 in simvastatin-treated wounds, and inflammatory cells had already diminished. The number of macrophages in simvastatin-treated wounds on day 7 was significantly

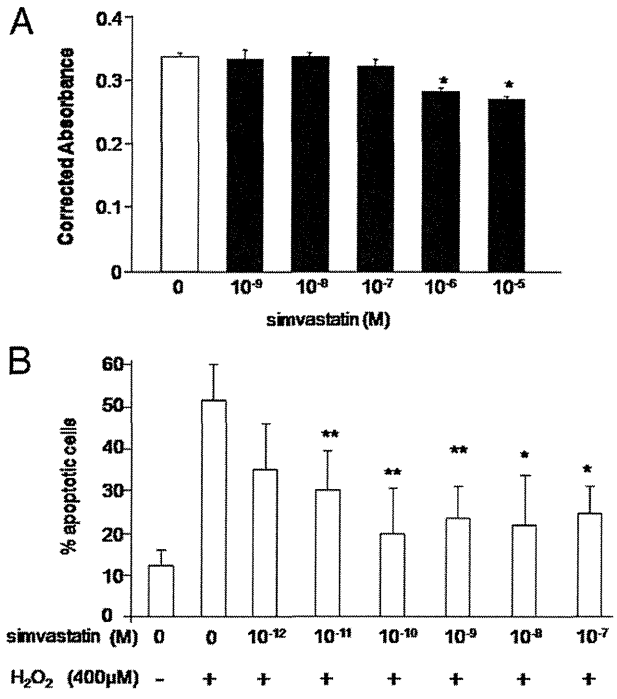

Figure 5. Effects of simvastatin on proliferation and apoptosis of LECs. **A:** Cell proliferation of LECs was investigated by MTS assay. Subconfluent cells (5000 cells per well) were reseeded on 96-well, flat-bottomed plates with 100 μL of growth media. The cells were treated with simvastatin and incubated for 48 hours at 37°C. Absorbance at 570 nm was recorded using a 96-well ELSIA plate reader. Quantification was performed as described in *Materials and Methods*. $^{*}P < 0.05$ versus vehicle ($n = 8$ from three independent experiments). **B:** Cell apoptosis in LECs was investigated by TUNEL assay. LECs were plated on chamber slides and placed in medium. Cells were stimulated by simvastatin and incubated for 24 hours with medium containing 400 μmol/L H_2O_2. Quantification of apoptotic cells was performed as described in *Materials and Methods*. $^{*}P < 0.05$, $^{**}P < 0.01$ versus H_2O_2 treatment ($n = 3$ from three independent experiments).

greater than that in controls (Figure 6, A and B). Most of the macrophages in the simvastatin-treated group expressed the M2 marker, IL-13, rather than the M1 marker, TNF-α, whereas most macrophages in the vehicle-treated group expressed TNF-α rather than IL-13 (Figure 6, C–F). The macrophages in the simvastatin-treated group produced VEGF-C (Figure 7A), and VEGF-C expression was significantly up-regulated in simvastatin-treated wounds compared with controls (Figure 7B). Other proangiogenic mediators in wound granulation tissue were evaluated by real-time PCR. Platelet-derived growth factor β, endothelial nitric oxide synthase, and fibroblast growth factor 2 were significantly up-regulated by simvastatin stimulation (see Supplemental Figure S2 at *http://ajp.amjpathol.org*).

Discussion

In this study, we found that topical application of simvastatin accelerated diabetic wound healing via promotion of angiogenesis and lymphangiogenesis. Many studies have reported that statins, including simvastatin, have strong angiogenic effects on vascular endothelial cells or placental stem cells and that these effects are mainly mediated by the PI3-kinase/Akt pathway,[11,22,23] although we note that other findings have also been reported[24] Consistent with these reports, abundant neovascularization and proangiogenic growth factors were observed in wounds treated with topical simvastatin in our *in vivo* study. Statins were originally introduced as systemic antihyperlipidemic drugs; however, a recent study has shown the value of topical simvastatin.[14] An advantage of topical application is that a suitable concentration of simvastatin can be applied without a risk of serious systemic adverse effects, such as rhabdomyolysis. Our results suggest that topical application of simvastatin could be a

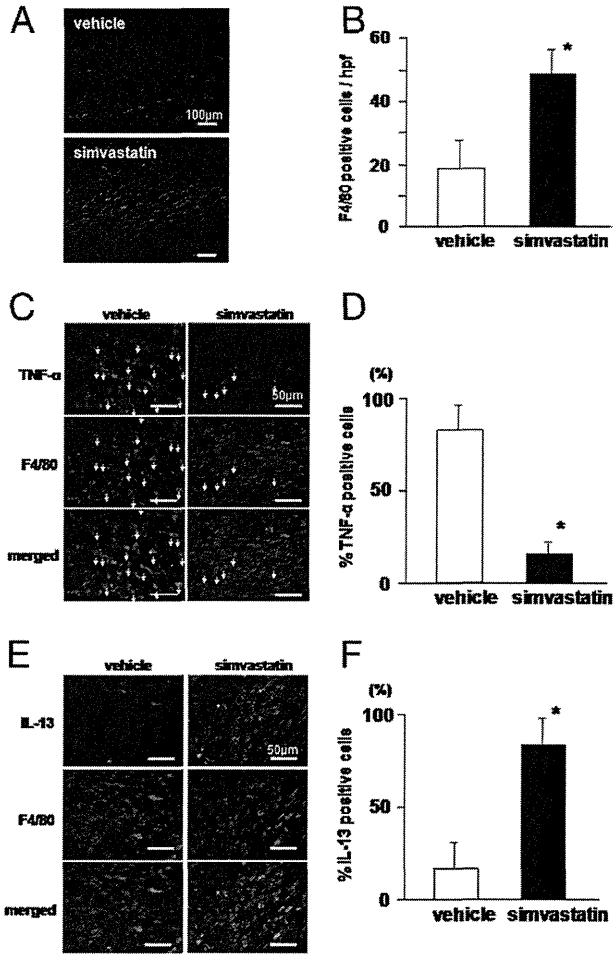

Figure 6. Effects of simvastatin on macrophage infiltration and phenotype in granulation tissue. **A:** Representative photomicrographs of the immunostained wound edge at 7 days after wound creation. Red fluorescence corresponds to F4/80-positive macrophages. Scale bar = 100 μm. **B:** The macrophage count, quantified as described in *Materials and Methods*. $^{*}P < 0.05$ versus vehicle ($n = 5$). **C:** Representative photomicrographs of the immunodetection of TNF-α and F4/80 in histologic sections from vehicle- or simvastatin-treated wounds (original magnification ×400). Scale bar = 50 μm. Green and red fluorescence corresponds to TNF-α–positive cells and F4/80-positive macrophages, respectively. Yellow indicates TNF-α–producing M1 phenotype macrophages (**white arrows**). **D:** Quantification of percentage of TNF-α–positive macrophages, as described in *Materials and Methods*. $^{*}P < 0.001$ versus vehicle ($n = 5$ in each group). **E:** Representative photomicrographs of immunodetection of IL-13 and F4/80 in histologic sections from vehicle- or simvastatin-treated wounds (original magnification ×400). Scale bar = 50 μm. Green and red fluorescence correspond to IL-13–positive cells and F4/80-positive macrophages, respectively. Yellow indicates IL-13–producing M2 phenotype macrophages. **F:** Quantification of percentage of IL-13–positive macrophages, as described in *Materials and Methods*. $^{*}P < 0.001$ versus vehicle ($n = 5$ in each group).

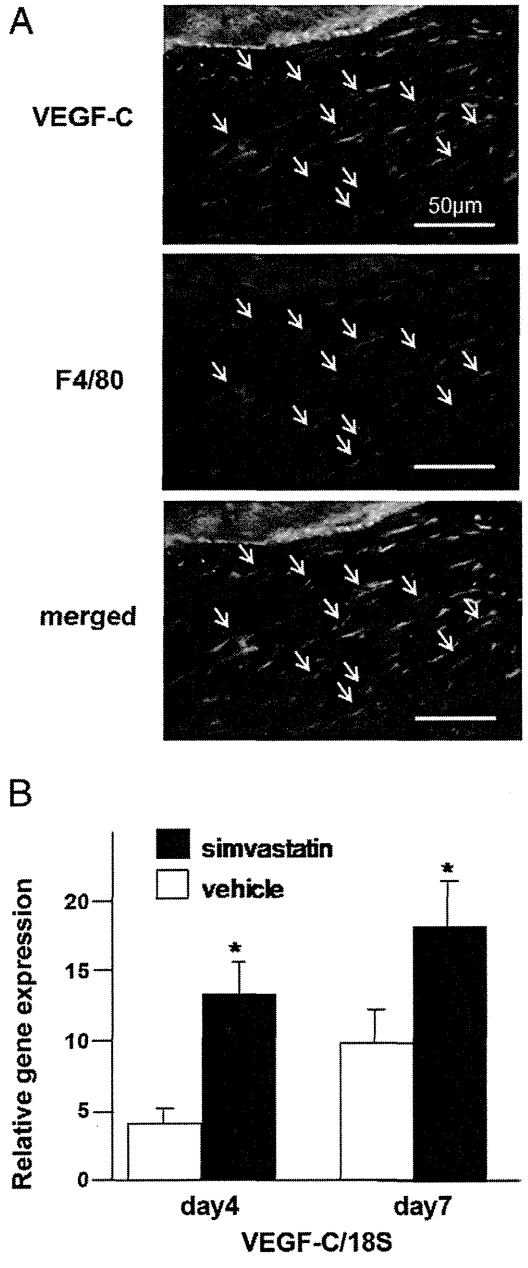

Figure 7. VEGF-C expression in granulation tissue. **A:** Representative photomicrographs of the immunostained wound edge treated with simvastatin at 7 days after wound creation. Green and red fluorescence indicates VEGF-C expression and F4/80-positive macrophages, respectively. Original magnification, ×400. **Arrows** indicate double-positive cells. Scale bar = 50 μm. **B:** Quantitative RT-PCR of VEGF-C in wound granulation tissue. Gene expression levels were normalized based on the level of an internal reference gene, 18S. $^*P < 0.05$ versus vehicle ($n = 5$).

new therapeutic strategy for treatment of local ischemic conditions, such as those in patients with diabetic ulcers.

Lymphangiogenesis is a major factor in diabetic refractory wound healing.[4,5] Therefore, we focused on the effects of simvastatin on wound lymphangiogenesis. Recent studies have suggested that several biological functions of LECs are partially regulated by the AKT/PI3K/mTOR pathway.[25,26] Consistent with these observations, capillary morphogenesis of LECs was significantly stimulated by simvastatin as an effect on vascular endothelial cells that was, at least in part, regulated by the AKT/PI3K/mTOR pathway. Our results suggest that the mechanisms underlying the lymphangiogenic effects of simvastatin in LECs might be similar to those for angiogenic effects. These mechanisms include antiapoptosis and promotion of capillary morphogenesis because LECs develop from a vascular network in an embryonic stage,[27] and these cells have a similar lineage. However, contrary to our expectation, simvastatin did not promote proliferation of LECs *in vitro*. During the wound healing process, new lymphatics are formed in newly generated granulation tissue, indicating that proliferation of preexisting lymphatic vessels is needed.

Because simvastatin did not promote the proliferation of LECs, we evaluated other possible sources of lymphangiogenic factors. Several reports suggest that infiltrating macrophages contribute to lymphangiogenesis as the major producer of VEGF-C in cutaneous wound healing,[4,5] and therefore we evaluated the effects of simvastatin on macrophages. Macrophages carry VEGF receptor 3, in addition to producing VEGF-C, and thus act as both autocrine and paracrine factors. We have previously reported that healing impairment in diabetes involves reduced lymphangiogenesis and suppressed macrophage function, such as recruitment to inflammatory sites and secretion of growth factors.[5] In this study, the number of infiltrating macrophages in granulation tissue was significantly increased by topical application of simvastatin, and most of these macrophages produced VEGF-C. These observations suggest that simvastatin recovers lymphangiogenic function that is impaired in macrophages under diabetic conditions.

Increased apoptosis is a major concern in wound healing in a diabetic state.[3,28–31] Hyperglycemia induces proinflammatory cytokines, such as TNF-α, and oxidative stress, which result in increased apoptosis in diabetes. Our study found that most infiltrating macrophages in diabetic wounds had an M1 proinflammatory phenotype producing abundant TNF-α. Simvastatin decreased H_2O_2-induced apoptosis in LECs *in vitro* and increased M2 anti-inflammatory phenotype macrophages in granulation tissue *in vivo*. We suggest that this anti-apoptotic effect of simvastatin also plays an important role, in addition to promotion of angiogenesis and lymphangiogenesis.

Increased infiltration of macrophages induced by simvastatin may have further benefits because the histologic scores of diabetic wounds were significantly improved by topical application of simvastatin. The histologic score reflects the degree of maturation of granulation tissue, including inflammation, collagen deposition, and reepithelialization, in addition to neovascularization. Macrophages play a central role in all stages of wound healing and orchestrate the wound healing process[32] by exerting proinflammatory functions and facilitating wound healing during the early stage and stimulating proliferation of fibroblasts, keratinocytes, and endothelial cells in the proliferative stage. Because the main focus of this study was lymphangiogenesis, we did not investigate the effects of simvastatin on reepithelialization or formation of extracellular matrix. This will require further experiments in a future study.

In conclusion, regulation of apoptosis and capillary differentiation are essential for development of functional lymphatics during wound healing. The findings of the present study suggest that topical simvastatin can stimulate lymp-

hangiogenesis directly and indirectly via stimulation of macrophages. Vascular remodeling induced by simvastatin might have therapeutic potential in patients with microvascular dysfunction, such as that in diabetic foot ulcer, a major cause of morbidity in the growing population of patients with diabetes. A future investigation is warranted to determine the potential clinical utility of this approach.

References

1. Jeffcoate WJ, Harding KG: Diabetic foot ulcers. Lancet 2003, 361: 1545–1551
2. Lerman OZ, Galiano RD, Armour M, Levine JP, Gurtner GC: Cellular dysfunction in the diabetic fibroblast: impairment in migration, vascular endothelial growth factor production, and response to hypoxia. Am J Pathol 2003, 162:303–312
3. Fadini GP, Albiero M, Menegazzo L, Boscaro E, Pagnin E, Iori E, Cosma C, Lapolla A, Pengo V, Stendardo M, Agostini C, Pelicci PG, Giorgio M, Avogaro A: The redox enzyme p66Shc contributes to diabetes and ischemia-induced delay in cutaneous wound healing. Diabetes 2010, 59:2306–2314
4. Saaristo A, Tammela T, Farkkila A, Karkkainen M, Suominen E, Yla-Herttuala S, Alitalo K: Vascular endothelial growth factor-C accelerates diabetic wound healing. Am J Pathol 2006, 169:1080–1087
5. Maruyama K, Asai J, Ii M, Thorne T, Losordo DW, D'Amore PA: Decreased macrophage number and activation lead to reduced lymphatic vessel formation and contribute to impaired diabetic wound healing. Am J Pathol 2007, 170:1178–1191
6. Oliver G, Detmar M: The rediscovery of the lymphatic system: old and new insights into the development and biological function of the lymphatic vasculature. Genes Dev 2002, 16:773–783
7. Witte MH, Bernas MJ, Martin CP, Witte CL: Lymphangiogenesis and lymphangiodysplasia: from molecular to clinical lymphology. Microsc Res Tech 2001, 55:122–145
8. Ji RC: Characteristics of lymphatic endothelial cells in physiological and pathological conditions. Histol Histopathol 2005, 20:155–175
9. Werner N, Nickenig G, Laufs U: Pleiotropic effects of HMG-CoA reductase inhibitors. Basic Res Cardiol 2002, 97:105–116
10. Landmesser U, Engberding N, Bahlmann FH, Schaefer A, Wiencke A, Heineke A, Spiekermann S, Hilfiker-Kleiner D, Templin C, Kotlarz D, Mueller M, Fuchs M, Hornig B, Haller H, Drexler H: Statin-induced improvement of endothelial progenitor cell mobilization, myocardial neovascularization, left ventricular function, and survival after experimental myocardial infarction requires endothelial nitric oxide synthase. Circulation 2004, 110:1933–1939
11. Kureishi Y, Luo Z, Shiojima I, Bialik A, Fulton D, Lefer DJ, Sessa WC, Walsh K: The HMG-CoA reductase inhibitor simvastatin activates the protein kinase Akt and promotes angiogenesis in normocholesterolemic animals. Nat Med 2000, 6:1004–1010
12. Bitto A, Minutoli L, Altavilla D, Polito F, Fiumara T, Marini H, Galeano M, Calo M, Lo Cascio P, Bonaiuto M, Migliorato A, Caputi AP, Squadrito F: Simvastatin enhances VEGF production and ameliorates impaired wound healing in experimental diabetes. Pharmacol Res 2008, 57:159–169
13. Emanueli C, Monopoli A, Kraenkel N, Meloni M, Gadau S, Campesi I, Ongini E, Madeddu P: Nitropravastatin stimulates reparative neovascularisation and improves recovery from limb ischaemia in type-1 diabetic mice. Br J Pharmacol 2007, 150:873–882
14. Otuki MF, Pietrovski EF, Cabrini DA: Topical simvastatin: preclinical evidence for a treatment of skin inflammatory conditions. J Dermatol Sci 2006, 44:45–47
15. Greenhalgh DG, Sprugel KH, Murray MJ, Ross R: PDGF and FGF stimulate wound healing in the genetically diabetic mouse. Am J Pathol 1990, 136:1235–1246
16. Asai J, Takenaka H, Katoh N, Kishimoto S: Dibutyryl cAMP influences endothelial progenitor cell recruitment during wound neovascularization. J Invest Dermatol 2006, 126:1159–1167
17. Asai J, Takenaka H, Kusano KF, Ii M, Luedemann C, Curry C, Eaton E, Iwakura A, Tsutsumi Y, Hamada H, Kishimoto S, Thorne T, Kishore R, Losordo DW: Topical sonic hedgehog gene therapy accelerates wound healing in diabetes by enhancing endothelial progenitor cell-mediated microvascular remodeling. Circulation 2006, 113:2413–2424
18. Abràmoff MD, Magalhães PJ, Ram S: J: image processing with ImageJ. Biophotonics Int 2004, 11:36–42
19. Jacobi J, Jang JJ, Sundram U, Dayoub H, Fajardo LF, Cooke JP: Nicotine accelerates angiogenesis and wound healing in genetically diabetic mice. Am J Pathol 2002, 161:97–104
20. Hirakawa S, Hong YK, Harvey N, Schacht V, Matsuda K, Libermann T, Detmar M: Identification of vascular lineage-specific genes by transcriptional profiling of isolated blood vascular and lymphatic endothelial cells. Am J Pathol 2003, 162:575–586
21. Maruyama K, Ii M, Cursiefen C, Jackson DG, Keino H, Tomita M, Van Rooijen N, Takenaka H, D'Amore PA, Stein-Streilein J, Losordo DW, Streilein JW: Inflammation-induced lymphangiogenesis in the cornea arises from CD11b-positive macrophages. J Clin Invest 2005, 115:2363–2372
22. Nakao T, Shiota M, Tatemoto Y, Izumi Y, Iwao H: Pravastatin induces rat aortic endothelial cell proliferation and migration via activation of PI3K/Akt/mTOR/p70 S6 kinase signaling. J Pharmacol Sci 2007, 105:334–341
23. Cantoni S, Cavallini C, Bianchi F, Bonavita F, Vaccari V, Olivi E, Frascari I, Tassinari R, Valente S, Lionetti V, Ventura C: Rosuvastatin elicits KDR-dependent vasculogenic response of human placental stem cells through PI3K/AKT pathway. Pharmacol Res 2012, 65:275–284
24. Zhao TT, Trinh D, Addison CL, Dimitroulakos J: Lovastatin inhibits VEGFR and AKT activation: synergistic cytotoxicity in combination with VEGFR inhibitors. PLoS One 2010, 5:e12563
25. Luo Y, Liu L, Rogers D, Su W, Odaka Y, Zhou H, Chen W, Shen T, Alexander JS, Huang S: Rapamycin inhibits lymphatic endothelial cell tube formation by downregulating vascular endothelial growth factor receptor 3 protein expression. Neoplasia 2012, 14:228–237
26. Dellinger MT, Brekken RA: Phosphorylation of Akt and ERK1/2 is required for VEGF-A/VEGFR2-induced proliferation and migration of lymphatic endothelium. PLoS One 2011, 6:e28947
27. Oliver G: Lymphatic vasculature development. Nat Rev Immunol 2004, 4:35–45
28. Hamed S, Ullmann Y, Egozi D, Daod E, Hellou E, Ashkar M, Gilhar A, Teot L: Fibronectin potentiates topical erythropoietin-induced wound repair in diabetic mice. J Invest Dermatol 2011, 131:1365–1374
29. Badr G: Supplementation with undenatured whey protein during diabetes mellitus improves the healing and closure of diabetic wounds through the rescue of functional long-lived wound macrophages. Cell Physiol Biochem 2012, 29:571–582
30. Ahmad J, Zubair M, Malik A, Siddiqui MA, Wangnoo SK: Cathepsin-D, Adiponectin, TNF-alpha, IL-6 and hsCRP plasma levels in subjects with diabetic foot and possible correlation with clinical variables: a multicentric study. Foot (Edinb) 2012, 22:194–199
31. Dave GS, Kalia K: Hyperglycemia induced oxidative stress in type-1 and type-2 diabetic patients with and without nephropathy. Cell Mol Biol (Noisy-le-grand) 2007, 53:68–78
32. Mahdavian Delavary B, van der Veer WM, van Egmond M, Niessen FB, Beelen RH: Macrophages in skin injury and repair. Immunobiology 2011, 216:753–762

Naoki Sasaki[1]
Mika Shinjo[1]
Satoshi Hirakawa[2]
Masahiro Nishinaka[3]
Yo Tanaka[3]
Kazuma Mawatari[3,4]
Takehiko Kitamori[3,4]
Kae Sato[1,4]

[1]Department of Chemical and Biological Sciences, Faculty of Science, Japan Women's University, Mejirodai, Bunkyo-ku, Tokyo, Japan
[2]Department of Dermatology, Hamamatsu University School of Medicine, Handayama, Higashi-ku, Hamamatsu, Shizuoka, Japan
[3]Department of Applied Chemistry, Graduate School of Engineering, The University of Tokyo, Hongo, Bunkyo-ku, Tokyo, Japan
[4]Core Research for Evolutional Science and Technology (CREST), Japan Science and Technology Agency, Kawaguchi, Saitama, Japan

Received December 14, 2011
Revised March 8, 2012
Accepted March 13, 2012

Research Article

A palmtop-sized microfluidic cell culture system driven by a miniaturized infusion pump

A palmtop-sized microfluidic cell culture system is presented. The system consists of a microfluidic device and a miniaturized infusion pump that possesses a reservoir of culture medium, an electrical control circuit, and an internal battery. The footprint of the system was downsized to 87 × 57 mm, which is, to the best of our knowledge, the smallest integrated cell culture system. Immortalized human microvascular endothelial cells (HMEC-1) and human umbilical vein endothelial cells (HUVEC) were cultured in the system. HMEC-1 in the system proliferated at the same speed as cells in a microchannel perfused by a syringe pump and cells in a culture flask. HUVEC in the system oriented along the direction of the fluid flow. Claudin-5, a tight junction protein, was localized along the peripheries of the HUVEC. We expect that the present system is applicable to various cell types as a stand-alone and easy-to-use system for microfluidic bioanalysis.

Keywords:
Endothelial cells / Orientation / Perfusion culture / Proliferation / Tight junctions
DOI 10.1002/elps.201100691

1 Introduction

Microfluidic devices are among the attractive platforms for cell separation, cell culture, and cell-based assays [1, 2]. For example, microfluidic devices have been utilized for hydrodynamic [3] and acoustophoretic [4] separation of cells. On the other hand, cell cultures and subsequent assay of cells in a microchannel have also been studied. The size of a microchannel is smaller than that of a cell culture flask, and the number of cells and amount of reagents utilized can therefore be reduced. Moreover, multiple microchannels and microchambers can be easily fabricated on a single device [5], and various applications such as fast and high throughput analyses by parallelization are expected.

Various types of cells have been cultured on microfluidic devices, such as endothelial cells located at the inner surface of blood vessels [6]. The size of the microchannel is comparable to that of blood vessels, and shear stress due to fluid flow is applied to the endothelial cells cultured in the microchannel. In fact, a number of microfluidic devices for vascular research have been reported. The devices have been applied to various experiments, including cell culture [7–10], cell adhesion assay [11, 12], shear stress response analysis [13–21], permeability measurement [22, 23], and transendothelial electric resistance (TEER) measurement [24, 25]. Another example of a cell cultured on microfluidic devices is the osteoblastic cell [26, 27]. The cell is responsive to shear stress due to fluid flow, which is easily controlled by channel dimensions and flow velocity. We have also developed cell-based microfluidic devices [28], and have reported a leukocyte adhesion assay on endothelial cells [29], recovery of cultured endothelial cells from a separable microfluidic device [30], and the automated long-term monitoring of alkaline phosphatase activity of osteoblastic cells [31].

Pumping of fluids into a microchannel is important for cell-based microfluidic devices. For example, it is necessary to pump medium for a perfusion culture and to introduce reagents for assays. Various pumping methods for cell-based microfluidic devices have been reported. Pumping by hydrostatic pressure is simple and has been utilized by various

Correspondence: Professor Kae Sato, Department of Chemical and Biological Sciences, Faculty of Science, Japan Women's University, 2-8-1 Mejirodai, Bunkyo-ku, Tokyo 112-8681, Japan
E-mail: satouk@fc.jwu.ac.jp
Fax: +81-3-5981-3661

Abbreviations: HMEC-1, immortalized human microvascular endothelial cells; **HUVEC**, human umbilical vein endothelial cells; **TEER**, transendothelial electric resistance

Colour Online: See the article online to view Fig. 5 in colour.

studies [8,11,13]. However, the pumping can induce only continuous flow. In contrast, a computer-controlled pump can induce various types of flow, including continuous flow and pulsatile flow, at various flow rates. Both a syringe pump and a peristaltic pump have been utilized for cell-based microfluidic devices. However, the commercially available pumps are generally larger than microfluidic devices, an aspect that limits downsizing of the whole system. An integrated culture system driven by a peristaltic pump has been reported [32], but it requires a large medium reservoir and a large motor controller compared to the device. Microfabricated peristaltic pumps have been utilized to analyze secreted molecules from cells [33] and to culture cells in microchambers in an automated manner [34]. However, these systems require additional valves and tubes to control the pumps, and the structure of the microfluidic devices becomes complex. A palm-sized cell culture system driven by Braille pins has been reported [35], but it requires external power supply for long-term culture (>2 h).

In this paper, we present a palmtop-sized, stand-alone cell culture system that consists of a microfluidic device and a miniaturized infusion pump. All the required components are integrated into the system, and there is therefore no need for tubes or electrical connections from outside the system. As a result, the footprint of the system can be downsized to 87 × 57 mm. We apply the system to culture both immortalized and normal endothelial cells in a microchannel. Then, we evaluate the culture in terms of proliferation rate, cell orientation under fluid flow, and expression of tight junction proteins. Control experiments are conducted with a microfluidic device and a syringe pump as examples of conventional microfluidic cell culture systems.

2 Materials and methods

2.1 Cells and culture procedures

Immortalized human microvascular endothelial cells (HMEC-1) [36] and human umbilical vein endothelial cells (HUVEC; Lonza, Basel, Switzerland) were selected as representatives of endothelial cell lines and normal human endothelial cells, respectively. HMEC-1 was cultured in a 25-cm^2 cell culture flask (353014, Becton, Dickinson and Company, Franklin Lakes, NJ, USA). The cells were grown in MCDB 131 (Invitrogen, Carlsbad, CA, USA) supplemented with 30% FBS (Invitrogen), 1×GlutaMAX™-I Supplement (Invitrogen), 13 μg mL^{-1} Hydrocortisone (Sigma-Aldrich, St. Louis, MO, USA), and 10 ng mL^{-1} epidermal growth factor (Sigma-Aldrich). HUVEC was cultured in a 25 cm^2 cell culture flask (3289, Corning, NY, USA). The cells were grown in EBM™-2 (Lonza) supplemented with EGM™-2 BulletKit (Lonza). All reported experiments utilized cells between passages 3 and 8.

Once cells reached confluence, the medium in a cell culture flask was aspirated. The cells were rinsed with 5 mL of PBS (TAKARA BIO, Shiga, Japan) and then treated with 500 μL of TrypLE™ Express (Invitrogen). After the cells were detached from the surface of the flask, 1 mL of fresh medium was added, and the obtained cell suspension was added to 4 mL of fresh medium in a 15-mL conical tube. The tube was centrifuged at 1200 rpm for 3 min and the supernatant was aspirated. Finally, the cells were resuspended in the medium at the required concentration.

2.2 Microfabrication

Microfluidic devices were fabricated using standard microfabrication techniques [37]. A negative master for the molding of PDMS was fabricated on a glass slide (S1226, Matsunami Glass, Osaka, Japan) with photoresist (SU-8 50, MicroChem, Newton, MA, USA). The master contained four I-shaped convex patterns, which gave recessed microchannel patterns (300 μm width, 67 μm depth, 20 mm length) to the PDMS part (2 mm thickness) after the molding. The surface of the master was passivated by coating with a fluoropolymer (INT-332VE, Noda Screen, Aichi, Japan). A prepolymer of PDMS (SILPOT 184, Dow Corning, Midland, MI, USA) was poured onto the master with a frame for holding the prepolymer. The prepolymer was cured in an oven at 65°C for 60 min, and the cured PDMS was peeled off from the master, bonded to a virgin glass slide, and cured again at 100°C for 60 min. Through -holes for tubes were punched at the end of the microchannel patterns on the PDMS part using a metal pipe. The PDMS part was then cut into four parts, each of which had the microchannel. Silicone tubes (0.5 mm id, 1.0 mm od, AS ONE, Osaka, Japan) or PTFE tubes (0.46 mm id, 0.92 mm od, NICHIAS, Tokyo, Japan) were glued to the through-holes with the prepolymer at 65°C for 60 min. The PDMS part with the tubes was sterilized in an autoclave at 121°C for 20 min, bonded to the bottom part of a 35-mm cell culture dish (Asahi glass, Tokyo, Japan), and kept in a clean bench until cell culture experiments.

2.3 Microfluidic cell culture systems

Figure 1A and B show microfluidic cell culture systems driven by a syringe pump (model 210, KD Scientific, Holliston, MA, USA). HMEC-1 was cultured in the system shown in Fig. 1A. One of the silicone tubes was connected to a 1-mL syringe (Terumo, Tokyo, Japan) via a metal pipe (0.33 mm id, 0.63 mm od, Nonaka Rikaki, Tokyo, Japan), a perfluoroalkoxy capillary (0.1 mm id, 0.3 mm od, Iwase, Kanagawa, Japan), and a needle (0.33 mm id, 0.63 mm od, Nonaka Rikaki). The other tube was connected to a capillary via a pipe. HUVEC was cultured in the system shown in Fig. 1B. One of the PTFE tubes was connected to a syringe via a bubble trap, a capillary, and a needle. The bubble trap was fabricated in accordance with details provided in the literature [38]. Two TYGON™ tubes (0.79 mm id, 2.38 mm od, Saint-Gobain K.K., Tokyo, Japan) and another TYGON tube (2 mm id, 4 mm od, Saint-Gobain K.K.) were used to compose the trap.

